



## REVIEW ARTICLE

# Recent advances in removal of toxic elements from water using MOFs: A critical review



Zeid Abdullah ALOthman<sup>a,\*</sup>, Muhammad Shahid<sup>b</sup>

<sup>a</sup> Department of Chemistry, College of Science, King Saud University, P.O. Box 2455, Riyadh 11451, Saudi Arabia

<sup>b</sup> Department of Environmental Sciences, COMSATS University Islamabad, Vehari 61100, Pakistan

Received 23 May 2022; accepted 27 September 2022

Available online 9 October 2022

## KEYWORDS

MOFs;  
PTEs;  
Adsorption;  
Wastewater;  
Reusability

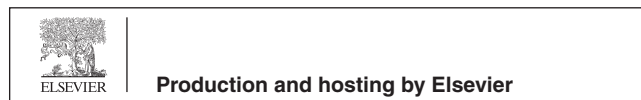
**Abstract** Water pollution with potentially toxic trace elements (PTEs) has seriously threatened the environment and human health globally. Their widespread occurrence at varied toxic levels and in different chemical forms has made remediation measures a cumbersome task. Furthermore, recent trends of PTE release via natural and/or human sources have further portended numerous detrimental events. Hence, effective remediation of PTE-contaminated aqueous media is highly substantial. Among various adsorbents, metal-organic frameworks (MOFs) have been recently characterized and tested being versatile and highly effective adsorbents for remediating pollutant/PTE-contaminated aqueous media. Owing to their plethora of structures and numerous intrinsic characteristics (high adjustability, porosity, surface area, selectivity, reusability, and structural stability), MOFs have lately received an obvious consideration in environmental remediation and analytical chemistry. This review initially summarized the most recent data (2018–2022) about PTE water contamination (rivers, lakes, canals, groundwater, city, and industrial wastewater). Then the review comprehensively highlighted the effects of synthesis techniques/conditions and post-synthetic functionalization's on MOF structural morphology by critically conferring the underlying mechanisms. Review summarizes MOF limitations apropos their large-scale industrial applications. The latest advancements regarding MOF syntheses and structural morphology to enhance their industrial applications have been updated and critically discussed. Likewise, the stability, selectivity, reusability, and multi-metal/pollutant removal potential of MOFs have been delineated using recent findings. Finally, the future perspectives have been put forth keeping in view the recent trends and potential research gaps. This review will act as guidelines for future studies of MOF-mediated PTE removal from wastewaters.

© 2022 The Authors. Published by Elsevier B.V. on behalf of King Saud University. This is an open access article under the CC BY-NC-ND license (<http://creativecommons.org/licenses/by-nc-nd/4.0/>).

\* Corresponding author.

E-mail address: [zaothman@ksu.edu.sa](mailto:zaothman@ksu.edu.sa) (Z.A. ALOthman).

Peer review under responsibility of King Saud University.



## 1. Introduction

During the last few decades, science has made tremendous progress along with fast growing industrialization. Simultaneously, the world population has grown rapidly in conjugation with unchecked and careless urbanization as well as improved living standards. All these factors have put a great pressure on the sustainability of natural resources. In fact, scientific and industrial advancements have resulted in the enhanced utilization of minerals in industrial processes and thereby the release of huge quantities of pollutants (inorganic, organic, organometallic, nanoparticles, gaseous pollutants, radioactive isotopes etc.) (Aldakhil et al., 2018; Aigbe and Osibote, 2021; Yuan et al., 2021; Li et al., 2022a).

Among different pollutants, environmental contamination with potentially toxic trace elements (PTEs) is a prevalent concern challenging scientists and researchers worldwide due to numerous concerns about the potential impact of these PTEs on environmental/human health (Shahid et al., 2018b). In fact, PTEs are among the most released environmental pollutants and are predominantly and commonly confronting environmental and human integrity. Some of the key PTEs include arsenic, chromium, manganese, mercury, lead, iron, cadmium, cobalt, nickel, copper, platinum, zinc, silver, tin, gold, vanadium, molybdenum, and titanium.

Studies have revealed the presence of these PTEs at supra-optimal levels in nearly all the environmental compartments (soil, air, water) (Shahid et al., 2018a). Among these, water contamination has emerged as a serious global issue. Water is one of the basic sources of life and mediates numerous key roles in human development and survival (Shahid et al., 2018b). Water contamination by different types of pollutants, especially PTEs, has received significant and widespread consideration (Shahid et al., 2018b; Natasha et al., 2021). This issue is even getting worse at a rapid pace with every passing day due to PTE release at substantial levels both by natural and anthropogenic sources (Table S1). The PTEs are extremely toxic pollutants and can induce various noxious effects on living organisms owing to their high toxicity. The PTEs have been reported to provoke a number of health disorders in the brain, kidney, liver, and immune system (Briffa et al., 2020).

Keeping in view the widespread contamination and potential toxic effects of PTEs, different health-related organizations have recommended threshold levels of these elements for drinking, irrigation, and domestic purposes. However, a great number of studies have revealed severalfold higher levels of these PTEs in aqueous media at a global scale (Table S1). Therefore, it has become evident that it is necessary to ensure safe limits of these pollutants are not surpassed in waters used for drinking or irrigation purposes. Remediation of PTEs from water is a cumbersome task due to their non-biodegradable nature compared to organic contaminants. Furthermore, due to the complex and varying compositions and conditions of natural waters, as well as the diverse nature of PTEs, successful remediation of these elements from waters remains extremely difficult to date.

Numerous methods, technologies, and materials have been explored to remove PTEs from aqueous media (Alqadami et al., 2020b; Ru et al., 2021; Shahid, 2021). Researchers have synthesized and characterized various materials which have been explored for their potential to remediate PTEs from water (Niazi et al., 2018; Ru et al., 2021). Nevertheless, effective remediation of these pollutants from aqueous media is still challenging and highly topical.

Recently, metal-organic frameworks (MOFs) have been established for their effective potential and various useful characteristics to remediate pollutants, including PTEs from water (Hu and Zhao, 2017; Alqadami et al., 2018b; Ru et al., 2021; Ji et al., 2022a). Still, numerous aspects and underlying mechanisms are not fully clear regarding MOF-mediated effective removal of PTEs from water. For instance, the effectiveness of different MOFs in terms of their stability, specific-and multi-PTE uptakes, and reusability are still contentious

under varied conditions. Similarly, the role of different factors which make an MOF adsorbent superior to another regarding pollutant/PTE remediation from aqueous media is not fully revealed. Likewise, the recent advancements in MOF synthesis and characteristics with respect to their industrial applications need to be summarized, updated, and discussed comprehensively.

This review therefore focuses on the status of water contamination by PTEs at a global scale (2018–22) and the use of MOFs as the emerging sorbents to effectively remove PTEs from contaminated waters. Based on recent literature data, this review critically discusses and compares the latest understanding regarding the (i) importance of synthesis materials/conditions and post-synthetic functionalization towards morphology and size of MOFs, (ii) factors affecting the stability of MOFs in aqueous media, (iii) selective adsorption of a specific PTE by MOFs, (iv) multi-PTE adsorption by MOFs, (v) reusability of MOFs to sorb PTEs, (vi) possible limitations of MOFs towards their industrial applications, and (vii) recent advancements in MOFs for their industrial applications.

## 2. Contamination of aqueous system by PTEs: Recent status and associated health risks

The PTEs are daily discharged to aqueous system from several anthropogenic and natural sources (Table S1, Fig. 1). Natural sources of PTE emissions to the ecosystem include volcanic eruptions, geogenic processes, and rock weathering. Anthropogenic PTE sources are related to activities of industry (metal processing and coal combustion), agriculture (sewage sludges, fertilizers, pesticides) and domestic (cosmetics, garbage, dust, detergents) (Briffa et al., 2020). The release of PTEs at huge amounts from different sources has negatively affected the water quality. Numerous reports have delineated high/toxic levels of various PTEs in surface water reservoirs (Natasha et al., 2020). Water contamination has been reported for all kinds of water resources (lakes, rivers, groundwater, city wastewater, industrial wastewater etc.) at a global scale.

Among the anthropogenic sources, mining plays a key role by generating and releasing huge quantities of PTEs (Briffa et al., 2020). Smelter emissions of PTEs are considered their main anthropogenic source and constitute about 40–73 % of the total anthropogenic PTE emissions (Liu et al., 2018; Briffa et al., 2020). Table 1 summarizes the annual mine production (2016–20) of some PTEs as reported by the USGS (USGS, 2021). Data reveals that each year, huge quantities of PTEs are mined and released into the environment.

A number of studies have revealed high levels of PTEs in water bodies due to mining activities. Obasi and Akudinobi (2019) showed high concentrations of various PTEs (Pb, Mn, Ni, Cr, Cd, Hg, Ag, As, Zn, Se, and Co) in water samples collected nearby a Pb–Zn smelter of Abakaliki, Nigeria. China produces and consumes the maximum quantities of nonferrous metals, and contributes significantly to environmental contamination. For example, 14.7 tonnes of Hg were released to the environment by the Zhuzhou Pb/Zn smelter during 1960–2011 (Wu et al., 2014). It is estimated that annually about 7000 tonne of Cd, 50000 tonne of Cr, and 60000 tonne of Ni may be emitted from various anthropogenic sources, especially mining (Ali et al., 2019).

Recent data reports that approximately 40 % of the lakes and rivers are contaminated by PTEs around the globe (Table S1) (Zhou et al., 2020a). This signifies a serious public issue owing to the toxic potential of PTEs. For example, Zhou et al. (2020a) assessed the PTE levels in rivers and lakes

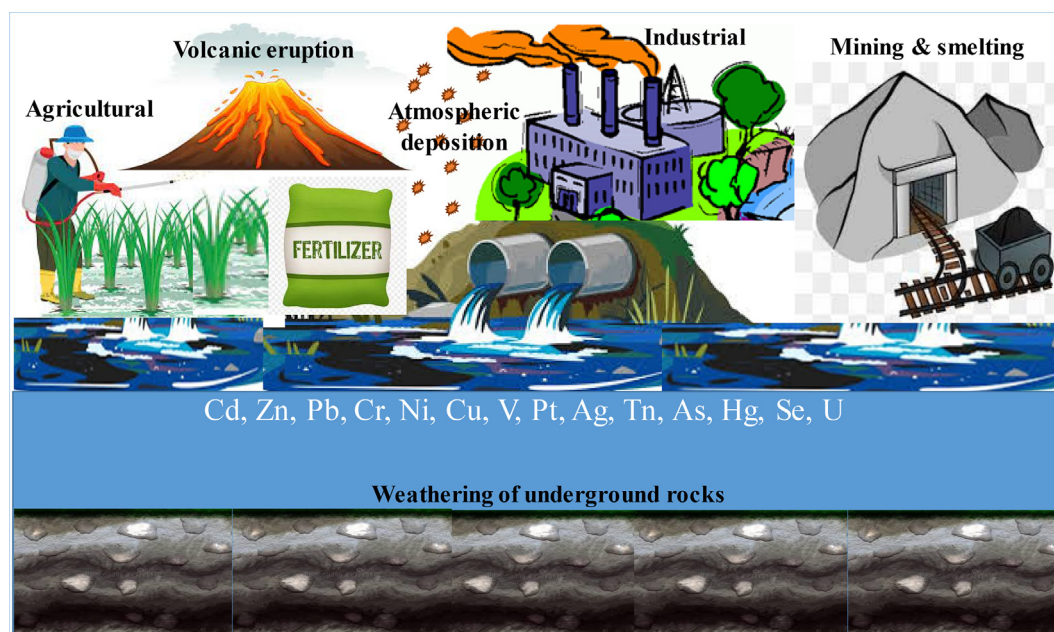


**Fig. 1** Various natural and anthropogenic sources of potentially toxic metal(loid)s in the environment.

**Table 1** Data about potentially toxic metal(loid) global mine production and % change in production during last 5 years. Source (USGS 2021, extracted on November 11, 2021) (USGS, 2021).

| Metal (loid) | 2016      | 2017      | % Change 2016–17 | 2018      | % Change 2017–18 | 2019      | % Change 2018–19 | 2020      | % Change 2019–20 |
|--------------|-----------|-----------|------------------|-----------|------------------|-----------|------------------|-----------|------------------|
| Sb           | 130       | 150       | 15               | 140       | -7               | 160       | 14               | 153       | -4               |
| As           | 36.5      | 37        | 1                | 35        | -5               | 33        | -6               | 32        | -3               |
| Cd           | 23        | 23        | 0                | 26        | 13               | 25        | -4               | 23        | -8               |
| Cr           | 30,400    | 31,000    | 2                | 36,000    | 16               | 44,000    | 22               | 40,000    | -9               |
| Co           | 123,000   | 110,000   | -11              | 140,000   | 27               | 140,000   | 0                | 140,000   | 0                |
| Cu           | 19,400    | 19,700    | 2                | 21,000    | 7                | 20,000    | -5               | 20,000    | 0                |
| Fe           | 1,360,000 | 1,500,000 | 10               | 1,500,000 | 0                | 1,500,000 | 0                | 1,500,000 | 0                |
| Pb           | 4820      | 4700      | -2               | 4400      | -6               | 4500      | 2                | 4400      | -2               |
| Mn           | 16,000    | 16,000    | 0                | 18,000    | 13               | 19,000    | 6                | 18,500    | -3               |
| Hg           | 4.5       | 2.5       | -44              | 3.4       | 36               | 4         | 18               | 3.7       | -8               |
| Ni           | 2250      | 2100      | -7               | 2300      | 10               | 2700      | 17               | 2500      | -7               |
| Zn           | 11,900    | 13,200    | 11               | 13,000    | -2               | 13,000    | 0                | 12,000    | -8               |
| Zr           | 1460      | 1600      | 10               | 1500      | -6               | 1400      | -7               | 1400      | 0                |

at a global scale during five time periods (1970s, 1980s, 1990s, 2000s, and 2010s). They reported that the levels of 2, 4, 8, 8, and 10 PTEs were higher than the threshold limits of USEPA and WHO, respectively, in the 1970s, 1980s, 1990s, 2000s, and 2010s. It means both the number and level of PTEs having their toxic environmental concentrations are increasing with time worldwide. Moreover, it was observed that the levels of PTEs were higher in developing countries (Africa, Asia, and South America) than in developed areas (Europe and North America) (Zhou et al., 2020a).

High levels of PTEs (such as Zn, Cu, and Cd) exceeding the permissible drinking water limits have been reported in nine Chinese rivers (Xu et al., 2017). In Bangladesh, almost all the major rivers (Karnaphuli, Buriganga, Turag, Sitalakhya, Balu, and Dhaleshwari rivers) are highly contaminated by different types of PTEs (Fe, Cu, Zn, Cd, Pb, Ni, Cr, and Mn)

(Uddin and Jeong, 2021). Even these rivers are causing groundwater pollution problems in Bangladesh due to seepage of polluted water into ground aquifers. Similarly, various PTEs (especially Sr and Al) have been reported in two major rivers of Turkey (Leventeli et al., 2019).

The contamination of rivers and lakes by PTEs is generally due to anthropogenic activities. In fact, >90 % of sewage water is discharged directly into water bodies without any treatment in developing countries (Natasha et al., 2020). The surface water reservoirs are considered easily accessible for discharge of sewage, and hence receive the maximum pollutants on a daily basis. Therefore, most of the lakes and rivers, especially those passing near the industrial zones or metropolitans of less-developed countries, are highly contaminated by different types of pollutants (Natasha et al., 2020; Long et al., 2021; Tong et al., 2021). It is envisaged that industrial activities dis-

charge about 300–400 megatons of waste into water reservoirs per annum (Boretti and Rosa, 2019). Similarly, most developing countries do not treat city wastewater and discharge it directly to water bodies (Natasha et al., 2020). According to an estimation, approximately 70–80 % of the total water used in household activities is released as wastewater (Kaur et al., 2012). The latest data available at FAO's AQUASTAT (AQUASTAT, 2022), reports that approximately 56 % of the total fresh water used is released in the form of wastewater globally. Based on available data by FAO states, it is reported that > 201 km<sup>3</sup>/year of wastewater is produced globally (excluding the data not available for several countries) (AQUASTAT, 2022).

Groundwater represents an important source of freshwater. However, in several parts of the world, groundwater is highly contaminated by different kinds of PTEs, especially As (Table S1) (Natasha et al., 2021). The weathering of metal (loid)-bearing minerals that are naturally present in the Earth's crust is the primary source of groundwater PTE contamination (Shahid et al., 2018b). Shaji et al. (2021) reported that > 90 % of Arsenic groundwater pollution is due to geogenic sources.

A number of recent studies have highlighted the issue of As groundwater contamination at global scale (Table S1). Recently, a few research reviewed groundwater status on a global scale and reported that groundwater contamination has spread to more than 70 countries. They reported that the most affected countries are situated in East Asia and South east Asia. While, Shaji et al. (2021) described that about 108 countries in the world are facing arsenic groundwater contamination. They predicted that > 230 million people are facing possible As poisoning worldwide. Among these 180 million people, the majority reside in Asia. The most As-affected countries include Bangladesh (85 million), India (50 million), Nepal (13 million), Pakistan (13 million), and Vietnam (10 million) (Shaji et al., 2021). Cao et al. (2021) developed a worldwide high As probability map of groundwater using 26 indicators and reported that > 70,612 data points at a global scale represent possible As contamination.

The contamination of water (any reservoir) can ultimately lead to human exposure to these toxic metal(loid)s. Many studies have reported human exposure to different kinds of PTEs, which can pose serious health hazards (Anwar et al., 2021; Shahid et al., 2021). Generally, PTEs are non-degradable with a potential to bioaccumulate, thereby always building up in the food chain and ultimately reaching humans (Anwar et al., 2021). At the same time, PTEs are highly persistent and can directly or indirectly provoke numerous noxious effects owing to biomagnification. A number of reports have revealed toxic accumulations of PTE in the food chain and possible associated health hazards (Shabbir et al., 2020a).

Several of these PTEs are highly toxic or even carcinogenic. The USEPA has classified numerous PTEs as priority pollutants. Some PTEs can induce serious toxic effects on multiple organs (lungs, prostate, skin, kidneys, stomach, liver, esophagus) of living organisms, even at low-exposed levels (Briffa et al., 2020). One of the key and initial pathways of PTE toxicity to living organisms is via oxidative stress (enhanced production of reactive radicals, thereby initiating oxidation of several substances/molecules) (Shahid et al., 2014b). Thus, water contamination by PTEs has become a severe dilemma and needs urgent and effective management and remediation at regional and global levels.

Keeping in view the possible exposure to PTEs, numerous organizations have recommended the threshold limits of these metal(loid)s in different environmental compartments, including water. These limits basically provide guidelines to avoid getting exposed to possibly toxic levels of these PTEs. As reported above, water reservoirs on a global scale contain PTE levels above these recommended values. Therefore, there is a dire need to establish highly effective technologies for the remediation of contaminated waters.

### 3. Technologies used for wastewater treatments

During the last few years, researchers have established various techniques to remediate PTEs from water (Naushad and Alothman, 2015; Alqadami et al., 2020a; Alomar et al., 2021; Tian et al., 2022; Zhang et al., 2022c). These technologies include coagulation, electrolysis, photocatalysis, membrane filtration, liquid extraction, biological treatments, chemical oxidation/reduction, and so on (Habiba et al., 2019; Naushad et al., 2019; Shabbir et al., 2020b). However, many of these techniques were not successful in effectively removing pollutants from water due to several associated issues. For instance, biological treatment is accompanied by the generation of secondary contaminants and a huge amount of sludge. These techniques have high energy and economic requirements, low removal potential, limited recycling, and the generation of large quantities of waste. Consequently, wastewater clean-up technologies have not been adopted in many areas around the globe, especially in less-developed regions.

In contrast to other techniques, adsorption is highly promising because of its high efficacy, flexible and simple design, cost efficiency, easy regeneration of a variety of adsorbents, ultra-low energy consumption, and minimal secondary pollution (Ghaedi, 2021). Adsorption is a key method that underlies numerous processes of high environmental and technological importance. The adsorption process mainly depends on the effectiveness and characteristics of adsorbent material. So far, different types of adsorbents have been widely used and reported in the literature. These adsorbents can be classified into (i) natural (clay, zeolite, siliceous material), (ii) industry-based (activated carbon, fly ash, ion-imprinted cryogel, waste sludge, alum waste, steel waste, red mud) (Soylak et al., 2017), (iii) bio-based (chitin, fungi, chitosan, algae, yeast) (Alothman et al., 2020) and (iv) agriculture-based (rice husk, moringa seeds, *Alium Cepa* seeds, *Senna auriculata* flowers, jujube seeds, almond shell, cassava peels, sawdust, groundnut shell, yam peel, tea waste, sugarcane bagasse, cotton stalks, watermelon rind, egg shell, corn cob, pomegranate peel, orange peel, banana peel, wheat straw, coconut shell etc.) (Niaz et al., 2018; Quyen et al., 2021; Tokay and Akpınar, 2021).

### 4. Metal organic frameworks: A recent class of effective sorbents

MOFs are a type of adsorbent that is distinguished by its effective removal of PTEs from water. The MOFs are a recently established class of crystalline porous materials that are considered highly effective next-generation adsorbents (Hu and Zhao, 2017; Yusuf et al., 2021; Alkas et al., 2022; Zhang et al., 2022a). Owing to their broad and pervasive potential applications, the syntheses, characterization, and use of MOFs

have become key research hot spots in several fields (Fuentes-Fernandez et al., 2018; Cui et al., 2020; Figueira et al., 2020; Forsyth et al., 2020; Gaikwad et al., 2021). Primarily, MOFs are an arrangement of metal ions (nodes) and organic ligands (linkers), which are connected in a specific order and interaction, thus resulting in the formation of a periodic network structure (Alqadami et al., 2018b; Ahmadijokani et al., 2021). Until now, various types of metal nodes have been recommended and used for MOF syntheses, such as Cu, Zr, Mn, Zn, Fe, Co, Cd, and Al. These metals are generally connected or bridged by different kinds of organic linkers such as amines, tetrazolates, carboxylates, sulfonates, etc.

This interaction of metal nodes and organic linkers results in the development of different types of geometric structures of MOFs including linear, square planar, T-/Y-shaped, pyramidal, cubic, trigonal, tetrahedral, and octahedral. Among these, the three-dimensional porous crystalline structure is the most common. MOFs with varied geometric structures can be synthesized due to great variation in the types of metal nodes, organic linkers, and reaction conditions. Hence, a great number of MOFs can be prepared by all the possible groupings/combinations of metal ions and organic binders.

Usually, recently prepared MOFs are known for their high surface area, great stability (thermal, chemical, water), highly organized pore size, very-low density, and enormous adsorption potential. The interaction of organic ligands and metal nodes helps to adjust their pore size (micropore to mesopore), and thereby to obtain a desired porosity and the final shape (Wang et al., 2022a). The periodic network porous structure and tunable physico-chemical characteristics of MOFs make them highly applicable and a unique class of adsorbents for a variety of pollutants, including PTEs (Hu and Zhao, 2017; Liu et al., 2022; Mohan et al., 2022; Zhang et al., 2022b). Therefore, several recent reports have characterized them as highly suitable materials for the remediation of various pollutants including PTEs (Table S2). Recent data revealed that MOFs can outnumber in both capacity and rate the benchmark adsorbents commonly used for wastewater remediation.

Compared to other adsorbents (agricultural, natural, industrial, biological), MOFs are equipped with the following advantages: (i) highly organized pore size, high surface area, great stability, and very-low density, (ii) higher PTE removal/adsorption capacity owing to their strong interactions (Hu and Zhao, 2017; Ahmadijokani et al., 2021; Zhao et al., 2021), and (iii) PTE adsorption/removal mechanism is more efficient and scientific (Ahmed and Jung, 2017; Zhao et al., 2021).

#### 4.1. MOF synthesis

Owing to their exceptional and diverse intrinsic properties, the synthesis of MOFs is gaining great importance for their various applications (Li et al., 2019; Rani et al., 2019; Kumar et al., 2020; Schernikau et al., 2021). The synthesis methods of MOFs govern their structure and thus the characteristics, effectiveness, and application of these porous materials (Srinivasan et al., 2020; Ru et al., 2021; Yusuf et al., 2021). Since their discovery, numerous MOF synthesis processes have been established, and improved to produce MOFs of desired structures, characteristics and uses. Several research and review articles have comprehensively discussed the synthesis

strategies of MOFs (Li et al., 2021; Zhao et al., 2021). The majority of MOF synthesis, including crystallization, is done in a solvo(hydro)thermal environment at high pressure and temperature. Typical MOF synthesis involves dissolving metal nodes and organic linkers in a solvent under a closed reaction vessel (Fig. 2).

There exist several classifications of MOF synthesis, such as diffusion, template synthesis, volatilization, ultrasonic, conventional electric heating, hydrothermal, solvothermal, electrochemical, microwave-assisted, sonochemical, and mechanochemical (Kobielska et al., 2018; Ghorbani-Choghamarani et al., 2021; Wang et al., 2021a). These methods are rapid and produce cleaner MOFs. These varied MOF synthesis techniques have mediated the development of hundreds of different types of MOFs. In addition to these methods, some specific synthesis techniques have been established to produce crystal size and shape, membranes, thin films, and numerous other structures made of MOFs (Khalil et al., 2022). The development of more sophisticated methods has made it easy to effectively govern and adapt desirable MOF morphology and size and thereby their allied functions and properties (Al-Wasidi et al., 2022; Hu et al., 2022b). Moreover, scientific advancements have improved MOF synthesis techniques from day-long techniques (such as solvothermal, hydrothermal, and sonochemical) to hourly-interval processes (such as co-precipitation) (Kumar et al., 2019).

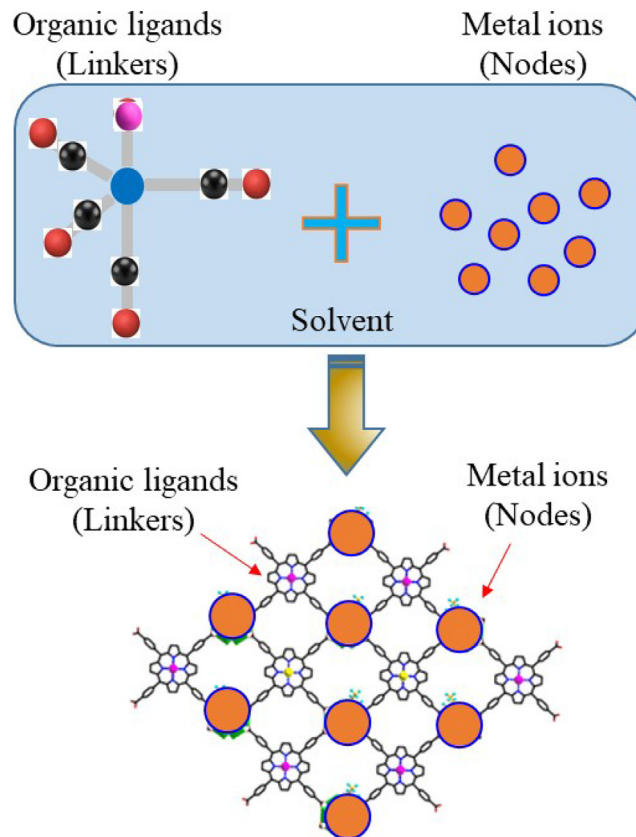


Fig. 2 Schematic MOF synthesis.

#### 4.2. Mechanisms involved in MOF-mediated PTE removal from wastewater

The MOFs have been successfully applied for the adsorption and purification of PTEs from water (Hu et al., 2022a; Omer et al., 2022). Table 2 describes recent data about MOF-mediated removal of PTEs from wastewaters. Apparently, several studies have reported effective PTE removal from aqueous using MOF under varied experimental conditions such as contact time, pH, temperature, and applied levels of MOFs and PTEs. These studies mainly reported the removal percentage and adsorption capacity (mg/g) of different MOFs for various PTEs under varied experimental conditions. It is evident that this class has a wide range of adsorbents already synthesized and has some adsorption mechanisms for different types of PTEs. The PTE adsorption potentials of MOFs range from

a few to hundreds of mg/g (Table 2, Table 2S). For example, Jiang et al. (2021b) demonstrated 719.42 mg/g (98 %) adsorption of Pb by Fe<sub>3</sub>O<sub>4</sub>@ZIF-8.

The literature data reveals that MOFs are, overall, highly effective at remediating a variety of PTEs from aqueous media under varied conditions of pH (Table S3), contact time (Table S4), and applied levels of MOFs (Table S5) and PTEs (Table S6). It is evident from literature findings that PTE adsorption by MOFs increases with enhancing applied conditions (up to certain levels until equilibrium is achieved). For example, Khalil et al. (2022) demonstrated 93.3 % (102.24 mg/g) Ce(III) adsorption on Co-MOF at pH 5.1. They reported that an increase in solution pH from 1.01 to 5.1 enhanced the distribution coefficient of Ce<sup>3+</sup> from 17.46 to 2791.30 ml/g. Gul Zaman et al. (2022) revealed that Pb adsorption by UiO-66-GMA increased from 22 % to 92 % by increasing pH from 1 to 6. However, a further increase in

**Table 2** Removal efficiency and/or adsorption capacity of various MOFs for PTE-contaminated wastewaters.

| Materials                                  | Metal | Q     | mg/g    | pH        | Reference                   |
|--|-------|-------|---------|-----------|-----------------------------|
| Fe <sub>3</sub> O <sub>4</sub> @ZIF-8      | Pb    | 98    | 719.42  | 1.0–7.0   | (Jiang et al., 2021b)       |
| Fe <sub>3</sub> O <sub>4</sub> @ZIF-9      | Cu    | 98    | 301.33  | 1.0–7.0   | (Jiang et al., 2021b)       |
| Cu-MOF-74                                  | Cd    | 95    | 150     | 6.5       | (Kim et al., 2021)          |
| Zr-MOF                                     | Cd    | –     | 37      | 3.0–9.0   | (Nimbalkar and Bhat, 2021)  |
| Zr-MOF                                     | Pb    | –     | 100     | 3.0–9.0   | (Nimbalkar and Bhat, 2021)  |
| ZIF-8                                      | Pb    | –     | 700     | –         | (Tanihara et al., 2021)     |
| MoS <sub>4</sub> -MOF                      | Hg    | 99.9  | –       | –         | (Yazdi et al., 2021)        |
| MIL-53(Al)-1                               | F     | –     | 75.5    | 1.0–12.0  | (Huang et al., 2021)        |
| Fe-MIL-88NH <sub>2</sub>                   | Pb    | 72.5  | 250     | 3.0–7.0   | (Fu et al., 2021)           |
| ZIF-8                                      | Pb    | 96    | 1780    | 2.0–12.0  | (Ahmad et al., 2021)        |
| ZIF-67                                     | Hg    | 94    | 1450    | 2.0–12.0  | (Ahmad et al., 2021)        |
| UiO-66-EDA                                 | Pb    | 99    | 243.9   | 2.0–9.0   | (Ahmadijokani et al., 2021) |
| UiO-66-EDA                                 | Cd    | 99    | 208.33  | 1.5–7.0   | (Ahmadijokani et al., 2021) |
| UiO-66-EDA                                 | Cu    | 99    | 217.39  | 1.5–7.0   | (Ahmadijokani et al., 2021) |
| Mag MOF-NH <sub>2</sub>                    | U     | 90.37 | 80      | 2.0–9.0   | (Chen et al., 2021)         |
| Cu-BTC                                     | Pb    | 85    | 230     | 2.0–6.0   | (Hasankola et al., 2019)    |
| Cu-BTC                                     | Hg    | 35    | –       | 2.0–6.0   | (Hasankola et al., 2019)    |
| ZIF-67/BC/CH                               | Cu    | –     | 200     | 2.0–6.0   | (Li et al., 2020a)          |
| ZIF-8/PAN                                  | Cu    | 96.14 | 250     | 2.0–6.0   | (Li et al., 2020a)          |
| PCN-221                                    | Hg    | 98    | 375     | 2.0–10.0  | (Hasankola et al., 2020)    |
| ZIF-67@Fe <sub>3</sub> O <sub>4</sub> @ESM | Cu    | 99    | 285     | 4.0–6.0   | (Mahmoodi et al., 2019)     |
| Zn(Bim)(OAc)-NS                            | Cu    | –     | 325     | 1.0–13.0  | (Xu et al., 2020)           |
| AMCA-MIL-53(Al)                            | Pb    | 79.5  | 390     | 1.47–8.13 | (Alqadami et al., 2018a)    |
| melamine-MOFs                              | Pb    | –     | 122     | 2.0–6.0   | (Yin et al., 2018)          |
| melamine-MOFs                              | Pb    | –     | 205     | 2.0–6.0   | (Yin et al., 2018)          |
| MOF-808-EDTA                               | La    | 99    | 205     | 2.0       | (Peng et al., 2018)         |
| MOF-808-EDTA                               | Pr    | 99    | –       | 2.0       | (Peng et al., 2018)         |
| ZIF-8                                      | Pb    | 99    | 1119.8  | 5.1       | (Huang et al., 2018b)       |
| Cu-MOFs/Fe <sub>3</sub> O <sub>4</sub>     | Pb    | 96    | 219     | –         | (Shi et al., 2018)          |
| La-MGs                                     | Sb    | 92.1  | 897.6   | –         | (You et al., 2022)          |
| MOF-199@PANI                               | Cu    | –     | 7831.34 | –         | (Yuan et al., 2022a)        |
| UiO-66-NH <sub>2</sub>                     | Cu    | –     | 364.96  | –         | (Hu et al., 2022a)          |
| UiO-66-NH <sub>2</sub>                     | Pb    | –     | 555.56  | –         | (Hu et al., 2022a)          |
| UiO-66-GMA                                 | Cu    | 96    | –       | –         | (Gul Zaman et al., 2022)    |
| Fe <sub>3</sub> O <sub>4</sub> @C-GO-MOF   | Pb    | –     | 344.83  | –         | (Wang et al., 2022b)        |
| Zr-MOFs                                    | Cu    | –     | 59.8    | –         | (Wang et al., 2018)         |
| ZnO-NP@Zn-MOF-74                           | Cu    | –     | 137.17  | –         | (Guo et al., 2021)          |
| Zr-MOF                                     | Cu    | –     | 79.34   | –         | (Subramaniam et al., 2022)  |
| ZIF-8                                      | Cu    | –     | 454.7   | –         | (Huang et al., 2018b)       |
| ZIF-8@GO                                   | Pb    | –     | 1119.80 | –         | (Li and Xu, 2021)           |
| Fe <sub>3</sub> O <sub>4</sub> @ZIF-8      | Cu    | –     | 719.42  | –         | (Jiang et al., 2021c)       |
| Fe <sub>3</sub> O <sub>4</sub> @ZIF-8      | Pb    | –     | 301.33  | –         | (Jiang et al., 2021c)       |
| CelloZIFPaper                              | Pb    | –     | 87.2    | 4         | (Abdelhamid et al., 2022)   |

**Table 3** Total pore volume and surface area of recently synthesized MOFs (2022 only).

| MOF  | Surface Area (m <sup>2</sup> /g) | Pore volume (cm <sup>3</sup> /g) | Reference                   |
|--|----------------------------------|----------------------------------|-----------------------------|
| UiO-66-NH <sub>2</sub>                                 | 576                              | 0.42                             | (Molavi et al., 2018)       |
| UiO-66-NH <sub>2</sub>                                 | 987                              | 0.51                             | (Zhu et al., 2019b)         |
| Zr-MOFs PW12@UiO-NH <sub>2</sub>                       | 977                              | 0.57                             | (Tian et al., 2018)         |
| UiO-66-NH <sub>2</sub> /GO                             | 822                              | 0.23                             | (Cao et al., 2018)          |
| UiO-66-NH <sub>2</sub>                                 | 963.8                            | 0.442                            | (Mansouri et al., 2021)     |
| UiO-66-NH <sub>2</sub>                                 | 1127                             | 0.48                             | (Gul Zaman et al., 2022)    |
| UiO-66-GMA   | 1045                             | 0.37                             | (Gul Zaman et al., 2022)    |
| ZIF-8  | 980                              | 0.44                             | (Abdelhamid et al., 2022)   |
| Cellulose: ZIF   | 100                              | 0.06                             | (Abdelhamid et al., 2022)   |
| ZIF-8@CP   | 230                              | 0.11                             | (Abdelhamid et al., 2022)   |
| ZIF-8@TOCNF  | 230                              | 0.14                             | (Abdelhamid et al., 2022)   |
| MIL-101(Cr)  | 3341                             | 1.80                             | (Keshavarz et al., 2022)    |
| MOF loaded-Cyanex                                      | 442                              | 0.19                             | (Keshavarz et al., 2022)    |
| MOF-HDEHP  | 1028                             | 0.47                             | (Keshavarz et al., 2022)    |
| MOF-TBP  | 1158                             | 0.57                             | (Keshavarz et al., 2022)    |
| Zr-MOF   | 295                              | 0.6                              | (Subramaniyam et al., 2022) |
| UiO-66-Cl  | 446                              | 0.274                            | (Yuan et al., 2022b)        |
| UiO-66-S   | 272                              | 0.237                            | (Yuan et al., 2022b)        |
| Fe <sub>3</sub> O <sub>4</sub> @ZIF-8                  | 160                              | 0.33                             | (Abdel-Magied et al., 2022) |
| Fe <sub>3</sub> O <sub>4</sub> @UiO-66-NH <sub>2</sub> | 287                              | 0.29                             | (Abdel-Magied et al., 2022) |

pH up to 9 decreased Pb adsorption by 70 % (please see further pH-related studies in Table S3). Similarly, UiO-66-GMA-mediated Cd adsorption increased from 90 to 95 % when contact times were enhanced from 1 to 200 min (Gul Zaman et al., 2022) (other time-based studies are listed in Table S4). Similarly, increasing the MOF dose (Zn-Ph-D CP) from 0.005 to 0.015 g/L increased Cu<sup>2+</sup> adsorption by 85–93 % (for more information, see Table S5). In case of PTE dose, Pb adsorption by CelloZIFPape increased from 205 to 750 mg/g with an increasing Pb initial level from 5 to 100 mg/L (Abdelhamid et al., 2022) (Table S6 highlights some other relevant studies).

The possible reasons/mechanisms of this effective PTE adsorption under diverse applied conditions can be; (1) the porous structure, high specific surface area, and pore volumes of MOFs assist increased diffusion of PTEs in the voids (Table 3) (Sheikhsamany et al., 2021; Zhao et al., 2021), and (2) more effective and controlled interaction mechanisms between PTEs and MOF active sites (Fu and Huang, 2018). There are several mechanisms of PTE adsorption on MOFs (Ru et al., 2021; Aljaddua et al., 2022). Generally, adsorption of a pollutant on MOF takes place via chemical or physical interactions between the porous structure and pollutants (Fig. 3). Some of the reported mechanisms for MOF-mediated PTE adsorption include: (i) coordination (Wang et al., 2017; Yuan et al., 2017; Wang et al., 2020b; Ru et al., 2021), (ii) electrostatic interactions (Cheng et al., 2020; Ahmadijokani et al., 2021; Esrafilii et al., 2021; Nqombolo et al., 2021), (iii) surface complexation (Zhao et al., 2020b; Ru et al., 2021) (iv) chelation (Wang et al., 2015b; Fu et al., 2019; Xiong et al., 2020; Ru et al., 2021), (v) hydrogen bonding (Daradmare et al., 2021; Ru et al., 2021), (VI) ion-exchange (Ke et al., 2018; Zhu et al., 2018; Nimbalkar and Bhat, 2021), and  $\pi$ - $\pi$  interaction (Pillai et al., 2019; Nqombolo et al., 2021) (Table 4).

The hard-soft-acid-base theory reveals that some PTEs interact with specific functional groups (hydroxyl, amino, phosphorous, sulphydryl, etc.) via chelation, electrostatic inter-

action, or ion exchange (Jeyaseelan et al., 2021c; Ru et al., 2021). Electrostatic interaction represents an attraction or repulsion between charged substances. Pillai et al. (2019) demonstrated the cationic and anionic electrostatic interaction between ZIF-8 and F. Efome et al. (2018) showed electrostatic interactions between Pb and MOF-300 and MOF-808 during the adsorption process. Kobielska et al. (2018) used FTIR and XPS data and suggested electrostatic interactions and hydrogen bonding between As<sup>5+</sup> and MIL-53(Al). Zhao et al. (2020b) revealed that electrostatic interaction and complexation helped UiO-66-NH<sub>2</sub> remove Pb from wastewater.

Ion exchange is a type of reversible chemical interaction in which a PTE from the aqueous medium replaces another ion from the surface of an MOF. Some studies reported ion exchange-based remediation of PTE-contaminated waters by MOFs (Ke et al., 2018; Zhu et al., 2018; Nimbalkar and Bhat, 2021). For instance, Goyal et al. (2021) revealed ion exchange remediation of Pb from water by Fe<sub>3</sub>O<sub>4</sub>-Cu-MOF (i-MOF). Similarly, Vilela et al. (2021) reported that K-exchanged Eu-based material showed a significant increase in the adsorption process.

Another interaction mechanism between PTEs and MOFs is hydrogen bonding, which is among the most frequently occurring chemical interactions in nature (Daradmare et al., 2021; Ru et al., 2021). Ahmed and Jhung (2017) reviewed the role of hydrogen bonds for the use of MOFs in adsorption and separation processes. They summarized a number of studies delineating hydrogen bonding for PTE adsorption on MOFs. Zhu et al. (2019a) reported that Pb adsorption on Tb-MOF was via the N-group due to synthesis of the inner-sphere complex (C-/=N···Pb).

#### 4.3. Effect of synthesis methods, materials, and conditions on MOF characteristics

The physico-chemical properties of MOFs linked with their structural morphology and size are primarily governed by the synthesis methods, materials, and conditions. The synthesis

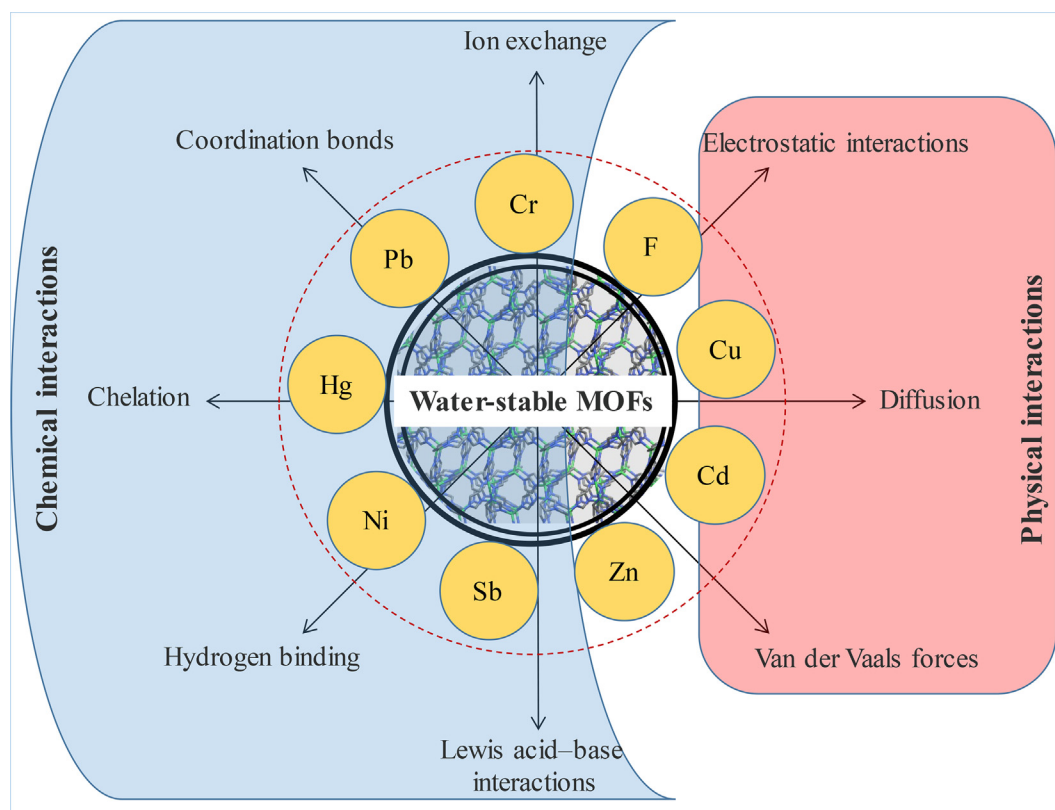


**Fig. 3** Possible physical and chemical mechanisms/interactions involved in potentially toxic metal(loid) adsorption on metal-organic frameworks (MOFs). Primarily, pollutants get adsorbed on MOF structure via chemical or physical interactions between the porous structure and pollutants. The most reported mechanisms of MOF-mediated PTE adsorption include coordination, electrostatic interactions, surface complexation, chelation, hydrogen bonding, ion-exchange, and  $\pi$ - $\pi$  interaction.

materials include the types of metal nodes, organic linkers, and reaction solvents. The synthesized MOFs can attain numerous coordination structural geometries depending on the synthesis material used (Orooji et al., 2020a; Xu et al., 2020; Soltani et al., 2021). For instance, the dimensionality and structural topology of an MOF rely on various coordination numbers and geometries that a metal node can adopt (Han et al., 2020). These coordination numbers and geometries vary with the type of metal ion used. This is the reason behind the use of transition metal ions for MOF synthesis due to their wide range of oxidation states and coordination numbers/geometries (Chiñas-Rojas et al., 2022). Hence, different structural morphologies have been reported for MOFs containing different types of metal nodes such as Zr, Co, Fe, Cu, Al, etc. (Table 2 and Table S2).

The type of organic linker primarily governs MOF structure. The commonly used organic linkers include O-donor or N-donor atoms. Organic linkers with N-donor atoms are represented by 4,4'-bipyridine. Such types of organic linkers may have 1–4 or even more N-donor atoms (Raptopoulou, 2021; Chiñas-Rojas et al., 2022). The selection of these different types of organic linkers with varied N-donor atoms is vital for attaining a specific pore size. Different types of organic linkers provide varied distances between the metal nodes. For example, replacing the 4,4'-bipyridine linker with pyrazine reduces the distance between the metal nodes and thus the porosity of the MOF (Chiñas-Rojas et al., 2022). In this

way, organic linkers can affect the pore size of MOFs and thereby the adsorption potential for PTEs.

Carboxylate ligands [RCO<sub>2</sub>] are linkers with O-donor atoms. This linker contains four-electron lone pairs at two O-donor atoms, which can be readily donated for the formation of coordination bonds (Chiñas-Rojas et al., 2022). Consequently, carboxylate ligands have appeared as one of the most abundant and versatile linkers in coordination chemistry. This difference in the coordination mode of O-donor and N-donor organic linkers greatly affects the structure of resulting MOFs, and thereby the remediation of PTE-contaminated waters (Chiñas-Rojas et al., 2022).

Likewise, the type of organic linker (such as rigid vs flexible) dictates the structural design of the resulting MOF. For example, the flexible linkers impart a wide range of options for the development of crystalline structures. Moreover, based on their charge, MOFs can be neutral, cationic and/or anionic ionic (Chiñas-Rojas et al., 2022). Azolate-based linkers result in the formation of ionic and neutral MOF structures depending on linker connectivity and metal coordination number/geometry. The resulting charge of an MOF greatly influences its potential to adsorb PTEs.

Mostly, MOF synthesis is carried out by interacting metal nodes and organic linkers in a liquid phase. The type and characteristics of a solvent also affect the morphology of the produced MOFs. In general, the solubility, reactivity, and redox potential of a solvent determine its choice for interaction reac-



**Table 4** Types of interactions between MOFs and PTEs (recent data literature 2018–21).

| MOF  | Metal  | Interaction type                           | Reference                         |
|--|--|--|-----------------------------------|
| UiO-66-EDA   | Pb, Cd, Cu   | Covalent and electrostatic                 | (Ahmadijokani et al., 2021)       |
| Fe-MIL-88B   | Sb <sup>3+</sup> , Sb <sup>5+</sup>  | Electrostatic                              | (Cheng et al., 2020)              |
| MOFs@Abs   | Cr <sup>6+</sup>   | Covalent/hydrogen bonding/electrostatic    | (Daradmare et al., 2021)          |
| DF-MOFs  | Cd <sup>2+</sup> , Cu <sup>2+</sup> , Cr <sup>2+</sup>                                       | Electrostatic                              | (Esrafil et al., 2021)            |
| BTC (M-BTC) MOFs                                   | Zr <sup>4+</sup> , Fe <sup>3+</sup> , Al <sup>3+</sup>                                       | Electrostatic                              | (Jeyaseelan et al., 2021c)        |
| Fe <sub>3</sub> O <sub>4</sub> @ZIF-8              | Pb <sup>2+</sup> , Cu <sup>2+</sup>  | Electrostatic                              | (Jiang et al., 2021a)             |
| UiO-66   | Cd, Pb   | Coordination/ionic interaction             | (Nimbalkar and Bhat, 2021)        |
| ZIF-67/ZIF-8                                       | As <sup>5+</sup> , Cr <sup>6+</sup>  | Electrostatic/ $\pi$ -anionic interaction  | (Nqombolo et al., 2021)           |
| MoS <sub>4</sub> -MOF                              | Hg <sup>2+</sup> , Pb <sup>2+</sup> , Ni <sup>2+</sup> , Cd <sup>2+</sup> , Zn <sup>2+</sup> | Lewis base                                 | (Yazdi et al., 2021)              |
| Zr-MOF)  | Hg <sup>2+</sup>   | Bonding interaction                        |                                   |
| Fe@ABDC MOF  | F <sup>-</sup>   | electrostatic                              | (Jeyaseelan et al., 2021b)        |
| MIL-96(RM)   | F <sup>-</sup>   | Ion exchange                               | (Wang et al., 2020c)              |
| Sn(II)-TMA MOF                                     | F <sup>-</sup>   | Electrostatic                              | (Ghosh and Das, 2020)             |
| UiO-66-ATA(Zr)                                     | Pb <sup>2+</sup>   | Chelation, ion-exchange, and Electrostatic | (Xiong et al., 2020)              |
| Fe <sub>3</sub> O <sub>4</sub> @UiO-66@UiO-67/CTAB | Cr <sup>6+</sup>   | Electrostatic                              | (Li et al., 2020b)                |
| MOFs (UiO-66-NH <sub>2</sub> )-DHAQ                | Pb <sup>2+</sup>   | Electrostatic/complexation                 | (Zhao et al., 2020a)              |
| ZIF-8  | F <sup>-</sup>   | Electrostatic                              | (Pillai et al., 2019)             |
| ZIF-8  | F <sup>-</sup>   | Anionic- $\pi$                             | (Pillai et al., 2019)             |
| ZIF-8  | F <sup>-</sup>   | Cationic- $\pi$                            | (Pillai et al., 2019)             |
| MOF-801  | F <sup>-</sup>   | Ion exchange                               | (Zhu et al., 2018)                |
| (CaFu) MOF   | F <sup>-</sup>   | Ion exchange                               | (Ke et al., 2018)                 |
| PAN/AlFu-10  | F <sup>-</sup>   | Electrostatic                              | (Karmakar et al., 2018)           |
| CelloZIFPaper                                      | Cd <sup>2+</sup> , Cu <sup>2+</sup> , Fe <sup>3+</sup> , Pb <sup>2+</sup> , Co <sup>2+</sup> | Coordination, electrostatic interactions   | (Abdelhamid et al., 2022)         |
| Dawsonite (NH <sub>2</sub> -MIL-53(Al))            | Cu <sup>2+</sup>   | Cation exchange & Innersphere complexation | (Li et al., 2020a)                |
| Zr-MOFs  | Cu <sup>2+</sup>   | Adsorption                                 | (Wang et al., 2018)               |
| Zn-MOF   | Cu <sup>2+</sup>   | Adsorption                                 | (Haftan and Motakef-Kazemi, 2021) |
| Zr-MOF   | Cu <sup>2+</sup>   | Adsorption                                 | (Subramaniyam et al., 2022)       |
| ZnO-NP@Zn-MOF-74                                   | Cu <sup>2+</sup>   | Adsorption                                 | (Guo et al., 2021)                |
| ZIF-8  | Cu   | Intra-particle diffusion                   | (Huang et al., 2018b)             |
| ZIF-8@GO   | Cu   | Coordination                               | (Li and Xu, 2021)                 |
| ZIF-8@GO   | Pb   | Coordination                               | (Li and Xu, 2021)                 |
| Fe <sub>3</sub> O <sub>4</sub> @ZIF-8              | Cu   | Ion-exchange                               | (Jiang et al., 2021c)             |
| Fe <sub>3</sub> O <sub>4</sub> @ZIF-8              | Pb   | Ion-exchange                               | (Jiang et al., 2021c)             |
| CelloZIFPaper                                      | Co   | Coordination, electrostatic interactions   | (Abdelhamid et al., 2022)         |

tion (Han et al., 2020). The type and characteristics of a solvent control the activation energy and thermodynamics of interactions. Furthermore, solvent can influence the interaction of the metal node with the organic linker, and thus the overall crystalline structure of MOFs. Even so, altering the total solvent volume affects the geometry of MOFs, and thereby their adsorption potentials (Raptopoulou, 2021).

In addition to synthesis materials, the experimental conditions of metal node interactions with organic linkers also affect the size and morphology of the resultant MOFs. Collectively, MOF synthesis is governed by various experimental conditions such as reaction temperature, time, pH, and reactant levels (Cao et al., 2018; Ding et al., 2019). In fact, these experimental conditions affect the interaction between metal nodes and organic linkers. There are possibilities of different types of

interactions between the metal nodes and organic linkers under varied applied conditions, which ultimately define the three-dimensional structure of MOF and hence the PTE adsorption potential (Wang and Cohen, 2009).

Metal nodes are shown to interact with organic ligands via hydrogen bonds and  $\pi$ - $\pi$  interactions, which contribute to the final MOF structure and properties. (Raptopoulou, 2021; Chiñas-Rojas et al., 2022). Moreover, these interactions create inner surfaces and cavities in the MOF structure, which are filled by ions and guest and/or solvent molecules. The size of cavities created defines the porous structure of MOFs (Raptopoulou, 2021; Chiñas-Rojas et al., 2022). The experimental conditions can affect the size and shape of the cavities created and morphology of MOFs. However, researchers are still trying to improve the size of the pores to improve MOF

adsorption potential using various synthesis methods and experimental conditions.

#### 4.4. MOF postsynthetic functionalization

Lately, the postsynthetic functionalization of MOFs has received much attention, which introduces exceptional characteristics to these porous materials and governs numerous applications (Orooji et al., 2021a; Ansarian et al., 2022) (Fig. 4). The MOFs can be functionalized using several techniques such as loading with a specific material, generating composites with other materials, introducing functional sites via metals and ligands, etc. (Han et al., 2020; Orooji et al., 2020b; Ibrahim et al., 2021; Orooji et al., 2021b) (Table 5). Several reports have highlighted the use of various additives to govern and control MOF crystallization. In this way, these technologies can introduce the required characteristics and functions to the resultant MOF.

Recently, Han et al. (2020) summarized different postsynthetic functionalization techniques used to govern MOF structure, such as deprotonation regulation synthesis (NH<sub>2</sub>-MIL-125(Ti) MOF), coordination modulation synthesis (HKUST-1, Zr-based MOFs), and surfactant modulation synthesis (ZIF-67 MOF). During these MOF synthesis techniques, the size and morphology of the MOF structure are controlled by adding additives during crystallization and (iii) adding surfactants during crystallization (Zhou et al., 2020a).

Similarly, MOF functionalization can be mediated by grafting of materials equipped with high numbers of active functional groups (Ji et al., 2021; Soltani et al., 2021). The introduction of functional groups with MOFs helps them to mediate a more effective chemical interactions with different pollutants such as PTEs. Likewise, alterations are introduced in organic linkers to enhance functional groups by substituting hydrogen atoms. Until now, various functional groups have been introduced in MOFs such as amino, bromo, nitro, carboxylic-acid, and polyethyleneimine (Ji et al., 2021; Ru et al., 2021; Soltani et al., 2021). The introduction of these ligands significantly modifies the physicochemical properties of MOFs without altering their crystal structure and topology (Han et al., 2020; Ji et al., 2021) (Table S7).

Some researchers functionalized MOFs by introducing nanoparticles (NPs) into the MOF structure (Ghorbani-Choghamarani et al., 2021). Incorporating NPs has been applied to enhance the adsorption and separation capacity of MOFs. For example, UiO-66 functionalized with NH<sub>2</sub>,

COOH, OH, and SO<sub>3</sub>H has a significantly higher adsorption capacity for PTEs (Han et al., 2020; Ru et al., 2021). Different combinations of NPs and MOFs have been explored to improve their adsorption potential (Ghorbani-Choghamarani et al., 2021).

Postsynthetic functionalization techniques also allow the synthesis of mixed-metal MOFs, possessing two or more metal nodes in their structure. The occurrence of additional metal nodes equips such MOFs with new and different characteristics (Ryu et al., 2021). Another approach to MOF functionalization is to expand their organic linkers to increase pore sizes. This technique provides sufficient space to enhance PTE diffusion into MOFs (Zhou et al., 2020a; Zhao et al., 2021). However, this technique compromises, in certain cases, the fundamental stability of the resulting MOFs.

Thus, using postsynthetic functionalization techniques, significant variations are possible in MOF structures such as porosity, topology, crystallinity, stability, and flexibility. This allows diverse and widespread MOF applications such as catalysis, adsorption, sensing, gas storage and capture, drug delivery, separation, and energy storage (Mallakpour et al., 2022). However, some studies also reported some defects in the MOFs after postsynthetic functionalization due to partial or complete replacement or absence of metal nodes and/or organic linkers. These defects in the crystalline structure of MOFs can greatly affect the functional characteristics and thereby the application of MOFs. Recently, Hou et al. (2022) revealed that besides different techniques of MOFs development, the strategy of functionalization and manufacturing defects in MOF can be another activation/modification technique of MOFs. However, the processes involved need to be controlled carefully to govern these functionalization and defects in MOFs.

Using these exceptional porous materials, researchers have synthesized composite membranes for various applications. During the last few years, there has been tremendous evolution of MOF membrane synthesis, and various membranes have been synthesized (MIL, HKUST-1, IRMOF, MOF-5, ZIF etc.) and tested for purification of water (Li et al., 2020b; Hu et al., 2021; Nimbalkar and Bhat, 2021; Sheikhsamany et al., 2021). It is reported that the membranes prepared from substrate-MOF materials possess higher affinity for PTEs compared to nanostructured porous materials.

Postsynthetic functionalization can enhance the number of active sites and thereby the PTE chelating/adsorption potential of MOFs (Zhu et al., 2019a; Zhao et al., 2021). Enhanced

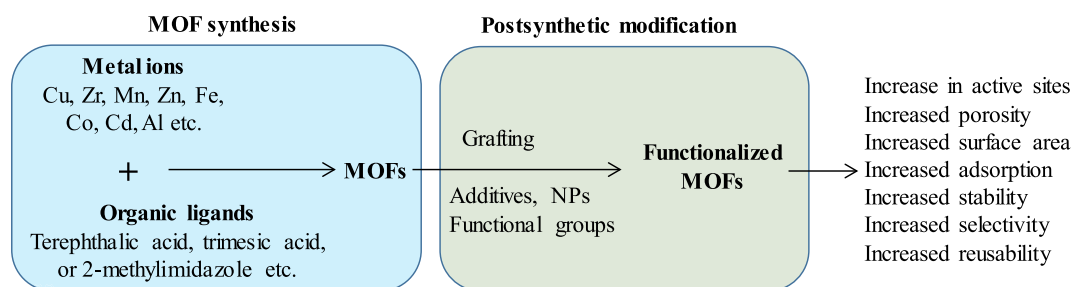


**Fig. 4** Schematic representation of MOF synthesis, post-synthetic functionalization and variation in MOF characteristics after MOF functionalization.

**Table 5** Effect of MOF postsynthetic functionalization on PTE adsorption.

| MOFs                   | Functionalized-MOF                | Functionalizing element   | PTE              | Adsorption | Purpose                  | Reference                   |
|------------------------|-----------------------------------|---|------------------|------------|--------------------------|-----------------------------|
| Zr-MOF                 | Form-UiO-66-NH <sub>2</sub>       | Formic acid and amino   | Cr <sup>6+</sup> | 338.98     | Selective removal        | (Chen et al., 2023)         |
| MIL-121                | carboxyl-MIL-121                  | carboxyl groups   | Cu <sup>2+</sup> | 99 %       | Selective removal        | (Ji et al., 2022b)          |
| MOF-808                | MOF-808-SH                        | Thioglycollic acid  | Hg <sup>2+</sup> | 977.5      | Selective removal        | (Ji et al., 2022a)          |
| UiO-66                 | UiO-66-EDA                        | Ethylenediamine   | Cu <sup>2+</sup> | 208.33     | Multimetal removal       | (Ahmadijokani et al., 2021) |
| UiO-66                 | UiO-66-EDA                        | Ethylenediamine   | Pb <sup>2+</sup> | 243.90     | Multimetal removal       | (Ahmadijokani et al., 2021) |
| UiO-66                 | UiO-66-EDA                        | Ethylenediamine   | Cd <sup>2+</sup> | 217.39     | Multimetal removal       | (Ahmadijokani et al., 2021) |
| MOF                    | TMU-81                            | Sulfonyl and amide groups   | Cd <sup>2+</sup> | 525        | Multimetal removal       | (Esrafil et al., 2021)      |
| UiO-66                 | UiO-66-NH <sub>2</sub>            | Amidinothiourea   | Au <sup>3+</sup> | 166.23     | Multimetal removal       | (Zhao et al., 2020c)        |
| MOF                    | Fe@BDC-MOF                        | Benzene-1,4-dicarboxylic acid   | F <sup>-</sup>   | 4.90       | Multimetal removal       | (Jeyaseelan et al., 2021c)  |
| MOF                    | Fe@ABDC                           | 2-aminobenzene-1,4-dicarboxylic acid                                  | F <sup>-</sup>   | 4.92       | Selective removal        | (Jeyaseelan et al., 2021c)  |
| UiO-66-(Zr)            | LDH/MOF NC                        | Ni <sub>50</sub> Co <sub>50</sub> -layered double hydroxide           | Hg <sup>2+</sup> | 509.8      | Multimetal removal       | (Soltani et al., 2021)      |
| UiO-66-(Zr)            | LDH/MOF NC                        | Ni <sub>50</sub> Co <sub>50</sub> -layered double hydroxide           | Ni <sup>2+</sup> | 441        | Multimetal removal       | (Soltani et al., 2021)      |
| UiO-66-NH <sub>2</sub> | CS grafted UiO-66-NH <sub>2</sub> | Chitosan  | Cu <sup>2+</sup> | 364.96     | Multimetal removal       | (Hu et al., 2022a)          |
| UiO-66-NH <sub>2</sub> | CS grafted UiO-66-NH <sub>2</sub> | Chitosan  | Pb <sup>2+</sup> | 555.56     | Multimetal removal       | (Hu et al., 2022a)          |
| UiO-66                 | UiO-66-SO <sub>3</sub> H          | SO <sub>3</sub> H   | Pb <sup>2+</sup> | 176.69     | Multimetal removal       | (Gul et al., 2022)          |
| UiO-66                 | UiO-66-SO <sub>3</sub> H          | SO <sub>3</sub> H   | Cd <sup>2+</sup> | 194.92     | Multimetal removal       | (Gul et al., 2022)          |
| Fe-MOF                 | PAN/MOFs                          | Polyacrylonitrile (PAN) and electrospun nanofibrous membranes (ENFMs) | Cr <sup>5+</sup> | 127.70     | Adsorption and reduction | (Miao et al., 2022)         |
| ZIF-8                  | MFZ-250                           | Fe <sub>3</sub> O <sub>4</sub> loading                                | Cd <sup>2+</sup> | 82         | Adsorption               | (Li et al., 2022b)          |
| ZIF-8                  | MFZ-500                           | Fe <sub>3</sub> O <sub>4</sub> loading                                | Cd <sup>2+</sup> | 103        | Adsorption               | (Li et al., 2022b)          |

selective removal of Hg (350.14 to 112.68 mg g<sup>-1</sup>) was obtained from water using UiO-66-NH<sub>2</sub> functionalized with L-cysteine (Feng et al., 2021a). Ahmed et al. (2019) revealed that UiO-66-COOH-ED (synthesized by UiO-66 functionalization with -NH<sub>2</sub> and -COOH groups) mediated 4.9-times increased adsorption of gadolinium ion (UiO-66-COOH-ED). While, other demonstrated 9 times higher Hg(II) removal in sewage by functionalizing Zr-MOFs with thiol. Detailed studies regarding postsynthetic functionalization in MOFs and remediation of PTEs have been listed in Table 5.

For a specific purpose such as PTE removal from water, functionalized MOFs may behave differently due to their numerous chemical and structural variations such as porosity, surface area, selectivity, reusability, and structural stability. Postsynthetic functionalization has resulted in the formation of MOFs that have a highly porous structure (up to 90 % of the crystalline volume), increased specific surface area (several thousand m<sup>2</sup>·g<sup>-1</sup>), potential to be recycled/regenerated (up to 10 cycles), enhanced selectiveness for a specific pollutant, and possess tremendous structural stability (thermal stability up

to 250–500 °C) accompanied by high pollutant removal efficiency. These characteristics distinguish one MOF from another when it comes to PTE removal from aqueous waters. However, different MOFs may be effective for different types of PTE. Studies have demonstrated that a wise choice of nodes, linkers, and functionalized materials can generate desirable MOFs for a specific purpose.

### 5. Limitations of MOFs for their industrial applications to remediate PTE-contaminated wastewater

Despite MOF-mediated efficient remediation of PTE-contaminated wastewaters, the industrial and large-scale applications of these adsorbents are still challenging due to numerous relevant limitations. Since their first synthesis, MOF-related research mainly focused on enhancing the surface area for increased adoption. However, during this quest, many MOFs synthesized were not capable for large-scale industrial application. The key limitations of MOFs in this regard include stability, specific PTE adsorption, multi-metal PTE

adsorption, production cost, possible toxicity to living organisms, mass production and regeneration potential.

### 5.1. Stability limitation

The industrial application of MOF greatly depends on its stability (water, chemical, and thermal) (Feng et al., 2018). Despite extraordinary performances of MOFs adsorbents to remediate different types of pollutants from water, the poor water stability is deterring their practical application. Degradation of an MOF after a prolonged exposure to humid conditions is not acceptable for their real-life applications. It is believed that to effectively remove PTEs and other pollutants from the aqueous media, the adsorbent used must have high water stability for possible future commercialization (Feng et al., 2018; Soltani et al., 2021).

Unfortunately, reports have characterized numerous MOFs being unstable in aqueous media such as MOF-511 and MOF-50812 (Batra et al., 2020). Majority of reported MOFs suffered from low endurance under aqueous media (Liu et al., 2020). Some studies revealed this water-sensitivity being the main shortcoming hindering practical MOF application of MOFs (Feng et al., 2018; Feng et al., 2021a; Soltani et al., 2021). The lifetime or stability of a compound is assessed using acceleration test under 85 % humidity and 85 °C temperature. Unfortunately, numerous previously synthesized MOFs were not able to sustain their structure due to their low aqueous acid/base stabilities (Ryu et al., 2021). Especially, Zn-based MOFs have been reported to breakdown easily after being exposed to humidity or chemicals (Ryu et al., 2021). Liu et al. (2020) reviewed and summarized numerous hydrophilic MOFs such as MIL-53(Cr), MIL-101(Cr), Cr<sub>3</sub>(BTC)<sub>2</sub>(Cr), BUT-8A(Cr), N<sub>3</sub>-PCN-333(Cr), MIL-53(Al), MIL-53- NH<sub>2</sub>(-Al), MUV-2(Fe), PCN-333(Fe), LaBTN(La), UiO-66(Zr), UiO-66- NH<sub>2</sub>(Zr), UiO-66-COOCu(Zr), UiO-67(Zr) and many more.

There are numerous underlying aspects that make an MOF hydrophilic and reduce its aqueous stability. Usually, the metal ion coordination bonding with linkers is prone to water attacks. In fact, exposure to water can displace MOF linkers, thereby mediating alterations in their structures. Thus, the governing parameters and underlying mechanisms of the intrinsic PTE-MOF adsorption properties and stability under varied humid, chemical, and thermal conditions need to be identified and improved.

### 5.2. Inefficient large-scale MOF synthesis

Another limitation apropos industrial application of MOFs is their low mass production. For large-scale industrial productions, a method needs to produce desired quality and quantity of required MOFs (Cai et al., 2021). Despite a great number of MOFs (> 100,000) being synthesized, the synthesis techniques usually yield < 1 g of high-quality porous crystalline material. There are numerous factors which overall govern the process of self-crystallization of MOFs. Hence, the optimization of crystallization process from small-scale to industrial scale is an uphill activity. Moreover, some processes such as solvent layering and vapor/base diffusion perform better under limited reaction volumes and are not ideal for large-scale production (Gao et al., 2021b; Ma et al., 2022). Similarly, high tempera-

ture and pressure requirements of certain methods are not easily viable at large scales. These restrictions of certain processes for mass production of MOFs are limiting their real-life applications.

### 5.3. Inefficient specific/selective PTE adsorption

In addition to MOF stability, efficiency of an MOF to effectively adsorb a specific PTE from aqueous media hinders its industrial commercialization. Selectivity process is considered the most important factor when assessing the application of a porous structure for water treatment (Sun et al., 2018; Goyal et al., 2021; Wu et al., 2021; Zhang et al., 2021a). The natural waters or wastewaters contain high amounts of competing ions (such as Ca, Mg, Na, and K), which can greatly interfere with the adsorption of a specific PTE by MOFs (Wang et al., 2020a; Goyal et al., 2021; Shamim et al., 2022). These competing ions block pores of crystalline structure, thereby affecting MOF capacity and/or removal rate. Therefore, it is of great importance that the MOFs must have selectivity preference for desired PTE over competing ions.

In industrial applications, MOFs are required to adsorb and remove a specific toxic substance (such as a PTE or a dye) from wastewater rather than other non-toxic substances. Under such conditions, the specific adsorption of a required PTE is highly vital for an effective remediation. Otherwise, the cost and quantity of waste material produced increased to a level making the technique ineffective. Consequently, the specific/selective adsorption of PTE from aqueous media have gained considerable attention in recent syntheses.

### 5.4. Inefficient multi-PTE adsorption

The syntheses of multifunctional adsorbents (such as the removal of more than one PTE or more than one pollutant) for wastewater remediation is still a mammoth challenge. Majority of the studies dealing with MOF-mediated PTE removal focused on a single PTE-contaminated aqueous media. In fact, these studies, in most cases, assessed the MOF-mediated PTE removal from a synthetic PTE solution prepared in a laboratory. The solvent used in these studies is generally a distilled water that is free from competing ions/metals. Only few studies have focused on MOF-mediated multi-PTE removal from naturally contaminated waters or industrial/municipal wastewaters (El-Hakam et al., 2021; Roy et al., 2021).

Although the presence of complex functional sites can significantly enhance PTM adsorption by adsorbents, many MOFs still adsorb only one or a few specific PTEs, but not all the co-existing PTEs. This scenario is more applied and crucial under natural conditions where waters, especially wastewaters are mostly contaminated with > one PTE. Therefore, it is highly imperative to develop adsorbents having strong binding strengths for diverse PTEs.

### 5.5. Inefficient regeneration/reuse of MOFs

One of the key features for a suitable industrial application of MOFs is their capacity of effective regeneration. This feature is highly important for energy saving and resource preservation. This characteristic is of great importance to minimize the

amount of waste produced and to manage MOF-related environmental toxicity. Briefly, regeneration of MOFs for their reuse to remediate PTE-contaminated waters helps to conserve resources, prevent pollution, and ensure economic feasibility.

### 5.6. Toxicity of MOFs

Another limiting factor vis-à-vis MOF industrial application is its potential toxicity. Despite considerable research, potential MOF toxicity to living organisms is poorly understood. Environmental sustainability demands complete understanding regarding the potential toxicity of a substance when released to ecosystem and tends to be exposed to living organisms. Some recent reports have highlighted MOF-induced toxic effects to living organisms due to the presence of PTEs and functional sites in MOFs (Ouyang et al., 2021; Ouyang et al., 2022). Generally, PTEs (Cd, Ni, Hg, Cu, Co, Zn etc.) are non-biodegradable and are present in MOFs in the form of NPs. Exposure to these PTEs via biomedical applications of MOFs can mediate numerous noxious effects in humans. Likewise, the organic linkers used to synthesize MOFs such as phosphonates, carboxylates, imidazolates, and amines can mediate moderate toxicity symptoms such as irritation. The solvents used (such as DMSO, DMF, and ethanol) for the liquid state reactions during MOF synthesis and the crystal size of MOFs may provoke toxicity to the organism exposed (Ouyang et al., 2022).

### 5.7. Synthesis cost of MOFs

One of the key factors mediating large-scale application and commercialization of a product is related to its production cost. The MOF synthesis cost is very high due to the use of numerous materials such as metal nodes, organic ligands, solvents, and catalysts. For example, Ryu et al. (2021) estimated the production cost of MOF-5, MOF-74 and UiO-66 approximately 527, 887 and 504 USD/kg. This makes MOF synthesis much costly than commonly used adsorbents such as agricul-

tural byproducts, silica gel, zeolites, and activated carbon, which have synthesis cost < 50 USD/kg. Hence, economic factors related to MOF synthesis are also limiting its industrial application.

## 6. Recent advancements in MOF synthesis and related mechanisms for improved industrial applications to remediate PTE-contaminated wastewaters

Keeping in view the vast considerations regarding the syntheses and applications of MOFs, these adsorbents have the potential to appear as a common material for daily use in coming years. Therefore, researchers/scientists are timely working on their future applications, especially at industrial scale. Hence, MOF synthesis processes have been improved and screened with time to improve and rectify their above-mentioned industrial limitations (Fig. 5). In this regard, various studies have reported numerous MOFs having ideal characteristics for their large-scale and industrial applications.

### 6.1. MOF stability and PTE removal from wastewater

Since the MOFs have been discovered, the synthesis realm has shifted from “water-sensitive” such as HKUST-1(Cu) and MOF-5(Zn) to “water-stable” such as MIL-101(Cr) and ZIF-8(Zn). Nowadays, MOFs are routinely designed to endure critical industrial conditions with paramount water stability such as UiO-66(Zr). Consequently, numerous water-stable MOFs have been synthesized and characterized for numerous applications including remediation of pollutants/PTEs from waters (Table 6). Various modifications have been made to MOF structures in recent past to improve their stability for pollutant removal from water (Feng et al., 2021a).

Water-stable MOF can preserve its structure and function under aqueous medium to govern possible interaction with PTEs. Lately, Batra et al. (2020) classified some recently-synthesized > 200 MOFs for their aqueous and kinetic stability using a machine learning-based model. For that, they used

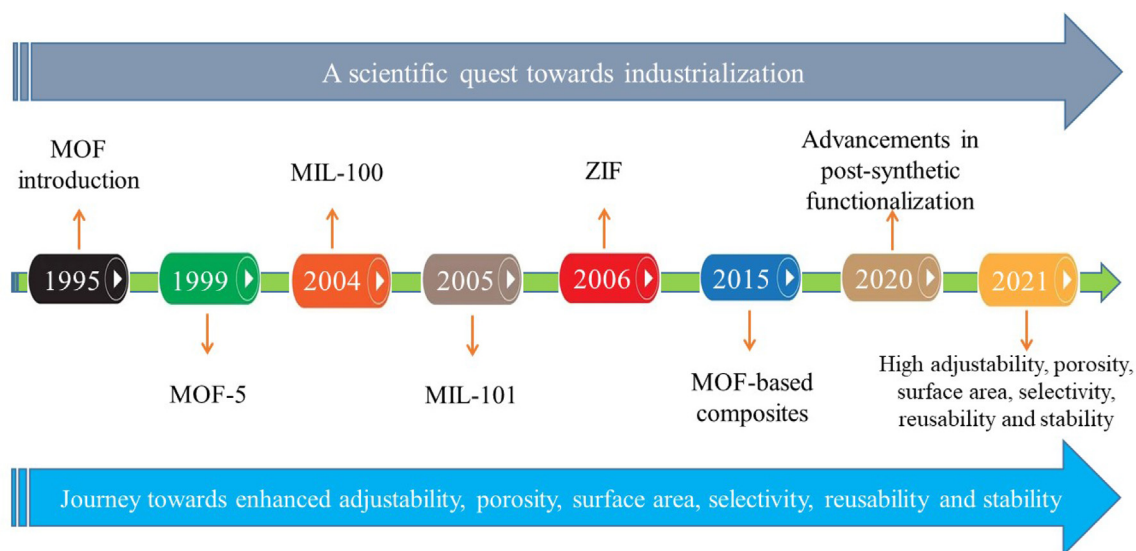


Fig. 5 Timeline of the historical MOF advancements towards possible industrialization [modified from Gao et al. (2021a)].

two types of models to classify MOFs (i) a two-class model to differentiate between stable and unstable MOFs, and (ii) a three-class model to classify MOFs as thermodynamically stable, kinetically stable, or unstable. The number of MOFs within each stability class were 25 stable, 118 having high kinetic stability, 42 with low kinetic stability and 22 unstable.

Several characteristics of an MOF determine its stability such as hydrophobicity, crystallinity, porosity, and coordination geometry of metal–ligand (Feng et al., 2018; Fu et al., 2019; Feng et al., 2021a). Moreover, the applied experimental conditions (pH, temperature) also affect MOF stability. Generally, the water stability of an MOF depends on coordination bonds between PTEs and organic ligands (Feng et al., 2018; Fu et al., 2019; Feng et al., 2021a). Hence, the strengths of the bonds that form MOF frameworks eventually determine the stability (Feng et al., 2018). The stronger the interaction bond between PTEs and organic ligands, higher will be the water stability of an MOF and vice versa. In fact, water molecules cannot substitute the strong bond existing between PTEs and organic ligands of an MOF.

The charge of metal cation positively correlates while the ionic radius negatively correlates with the strength of metal–ligand bond and thereby the stability of MOF (Devic and Serre, 2014; Ibrahim et al., 2021). Therefore, PTE ions with high charge densities (combined influence of metal ion charge and radius) form strong coordination bonds, and thereby stable MOFs. For example, the coordination of hard bases (such as carboxylate-based ligand) with high-valent PTE ions ( $\text{Al}^{3+}$ ,  $\text{Fe}^{3+}$ ,  $\text{Cr}^{3+}$ ,  $\text{Ti}^{4+}$ ,  $\text{Zr}^{4+}$ ) results in the formation of stable frameworks (Devic and Serre, 2014). Using these combinations of hard bases and high-valent PTEs, numerous stable MOF have been synthesized and applied for pollutant removal from water (Shahid et al., 2014a). These stable MOFs (MIL-100, MAFs, ZIF, UiO-66, UiO-67, MIL-101(Cr), NiCo-LDH/MO etc.) possess outstanding chemical stability for efficient pollutant remediation (Liu et al., 2020). Similarly, ligand with high acid dissociation constant (azoles) form strong interactions with low valent-PTE ions. Likewise, coordination of soft divalent PTE (such as Cu, Zn, Ni, Ag) with soft azolate ligands (triazolates, tetrazolates) generally forms stable structures (Ding et al., 2019; Ibrahim et al., 2021).

**Table 6** Examples of stability and regeneration/reuse potential of MOFs to adsorb PTEs from wastewaters (recent data literature 2018–21).

| Materials  | Metal            | # of cycles | Removal (%) | Adsorption (mg/g) | Reference                   |
|--|------------------|-------------|-------------|-------------------|-----------------------------|
| UiO-66-EDA   | $\text{Pb}^{2+}$ | 4           | 95–85       | –                 | (Ahmadijokani et al., 2021) |
| UiO-66-EDA   | $\text{Cd}^{2+}$ | 4           | 89–78       | –                 | (Ahmadijokani et al., 2021) |
| UiO-66-EDA   | $\text{Cu}^{2+}$ | 4           | 79–68       | –                 | (Ahmadijokani et al., 2021) |
| Mag MOF-NH <sub>2</sub>                                  | $\text{U}^{6+}$  | 5           | 90–88       | –                 | (Chen et al., 2021)         |
| Fe-MIL-88NH <sub>2</sub>                                 | $\text{Pb}^{2+}$ | 4           | 94–85       | –                 | (Fu et al., 2021)           |
| Zr-BTC   | $\text{F}^-$     | 8           | 98–68       | –                 | (Jeyaseelan et al., 2021a)  |
| Fe-BTC   | $\text{F}^-$     | 8           | 96–69       | –                 | (Jeyaseelan et al., 2021a)  |
| Al-BTC   | $\text{F}^-$     | 8           | 92–66       | –                 | (Jeyaseelan et al., 2021a)  |
| $\text{Fe}_3\text{O}_4$ @ZIF-8                           | $\text{Pb}^{2+}$ | 4           | 99–54       | –                 | (Jiang et al., 2021c)       |
| $\text{Fe}_3\text{O}_4$ @ZIF-8                           | $\text{Cu}^{2+}$ | 4           | 98–51       | –                 | (Jiang et al., 2021c)       |
| $\text{Fe}_3\text{O}_4$ @ZIF-8                           | $\text{Pb}^{2+}$ | 4           | –           | 340–175           | (Jiang et al., 2021c)       |
| $\text{Fe}_3\text{O}_4$ @ZIF-8                           | $\text{Cu}^{2+}$ | 4           | –           | 290–175           | (Jiang et al., 2021c)       |
| Cu-MOF-74  | $\text{Cd}^{2+}$ | 3           | –           | 85–64             | (Kim et al., 2021)          |
| Zr-MOF   | $\text{Pb}^{2+}$ | 3           | 26–17       | –                 | (Nimbalkar and Bhat, 2021)  |
| Zr-MOF   | $\text{Cd}^{2+}$ | 3           | 18–10       | –                 | (Nimbalkar and Bhat, 2021)  |
| ZIF-67/ZIF-8   | $\text{As}^{5+}$ | 5           | –           | 71–66             | (Ngombolo et al., 2021)     |
| ZIF-67/ZIF-8   | $\text{Cr}^{6+}$ | 5           | –           | 69–65             | (Ngombolo et al., 2021)     |
| Zr-MOF   | $\text{Hg}^{2+}$ | 3           | 98–84       | –                 | (Yan et al., 2022)          |
| ZIF-8@SnO <sub>2</sub> @CoFe <sub>2</sub> O <sub>4</sub> | $\text{Ni}^{2+}$ | 5           | –           | 12.3–9.3          | (Roudbari et al., 2021)     |
| Fe/Mg-MIL-88B  | $\text{As}^{5+}$ | 5           | 99–85       | –                 | (Zhou et al., 2020b)        |
| PCN-221  | $\text{Hg}^{2+}$ | 3           | 93–75       | –                 | (Hasankola et al., 2019)    |
| UiO-66-NH <sub>2</sub> @CA                               | $\text{Cu}^{2+}$ | 5           | 89–70       | –                 | (Lei et al., 2019)          |
| melamine-MOFs  | $\text{Pb}^{2+}$ | 5           | –           | 120–82            | (Yin et al., 2018)          |
| Cu-MOFs/Fe <sub>3</sub> O <sub>4</sub>                   | $\text{Pb}^{2+}$ | 5           | 96–50       | –                 | (Shi et al., 2018)          |
| UiO-66-GMA   | $\text{Pb}^{2+}$ | 5           | 94–78       | –                 | (Gul Zaman et al., 2022)    |
| UiO-66-GMA   | $\text{Cd}^{2+}$ | 5           | 98–81       | –                 | (Gul Zaman et al., 2022)    |
| MIL-121  | $\text{Pb}^{2+}$ | 10          | 99          | –                 | (Ji et al., 2022b)          |
| MIL-121  | $\text{Ni}^{2+}$ | 10          | 99          | –                 | (Ji et al., 2022b)          |
| MOFs   | $\text{Pb}^{2+}$ | 3           | 55–40       | –                 | (Zheng et al., 2021)        |
| MOFs   | $\text{Cr}^{6+}$ | 3           | 73–60       | –                 | (Zheng et al., 2021)        |
| UiO-66-S   | $\text{Fe}^{3+}$ | 6           | 99–89       | –                 | (Yuan et al., 2022b)        |
| CelloZIFPaper  | $\text{Pb}^{2+}$ | 3           | 99–89       | –                 | (Abdelhamid et al., 2022)   |
| CelloZIFPaper  | $\text{Cu}^{2+}$ | 3           | 99–60       | –                 | (Abdelhamid et al., 2022)   |
| CelloZIFPaper  | $\text{Co}^{2+}$ | 3           | 99–50       | –                 | (Abdelhamid et al., 2022)   |
| TMU-81   | $\text{Cd}^{2+}$ | 5           | 45–38       | –                 | (Esrafilii et al., 2021)    |
| UiO-66-ATU   | $\text{Au}^{3+}$ | 4           | 90–72       | –                 | (Zhao et al., 2020c)        |
| MFZ  | $\text{Cd}^{2+}$ | 4           | 99.9–78     | –                 | (Li et al., 2022b)          |

The characterization and applications of UiO-66(Zr) in numerous studies have revealed this MOF being high stable (Liu et al., 2020). This cubic close packed MOF has been synthesized using  $Zr_6O_4(OH)_4$  and carboxylate. The high stability of UiO-66(Zr) in aqueous medium depends on its high connectivity, which renders steric shielding to crystalline structure. Similarly, MIL-125(Ti) is another model of high-water stability.

MOF stability can also be increased by protecting the coordination sites from water attack. Adding alkyl functional groups or hydrophobic fluorinated to linkers can block water access to coordination bonds, thereby improving water stability of MOF structure. The water stability of UiO-67(Zr) improved significantly after incorporation of Trifluoromethyl groups. Several other studies also reported enhanced MOF water stability due to decorating different groups on MOF linkers.

Studies have proposed several other techniques to improve MOF chemical stability such as presence of hydrophobic skeleton, increasing ligand basicity and enhancing coordination numbers (Burtch et al., 2014; Ahmed and Jung, 2017). Similarly, enhancing the hydrophobicity of MOF internal surfaces also increases its stability (Ahmed and Jung, 2017). Functionalization of ligands also mediates stability to MOFs in water

(Wang and Cohen, 2009). The UiO-66-MOFs and their composites are highly water-stable due to short chains of ligands and strong coordinated bonds, which impart them excellent chemical and water stability. Recently, Morcos et al. (2021) reported that UiO-67 and UiO-66 MOFs sustained their structural stability after 95 % removal of Pb and was fully regenerated during four cycles.

### 6.2. Selective PTE removal efficiency of MOFs: Effect of competing ions

Selectivity process is considered the most important factor when assessing the application of a porous structure for water treatment (Table 7) (Sun et al., 2018; Goyal et al., 2021; Wu et al., 2021). Some studies have reported selectivity for certain PTE by MOFs despite high levels of competing ions: Hg(II) by MOF-808 (Ji et al., 2022a), Pb and Cu by MOF-2 (Cd) (Ghaedi et al., 2018), Cd and Hg by FJI-H9 (Xue et al., 2016), Pb and Hg by Fe-BTC/PDA (Sun et al., 2018), Pb by  $Fe_3O_4$  – Cu-MOF (i-MOF) (Goyal et al., 2021), and Pb by MIL-100 (Fe) (Zhang et al., 2021b).

There are different mechanisms of this PTE selectivity by MOFs over competing ions. One mechanism relies on Pearson's Hard-Soft-Acid-Base rule. Some metals (such as Cu

**Table 7** Examples of MOF-based selective removal of PTEs from wastewaters (recent data literature 2020–21).

| Materials  | Metal | Removal (%) | Adsorption (mg/g) | Time (min)    | Reference                     |
|--|-------|-------------|-------------------|---------------|-------------------------------|
| MOF-808-SH   | Hg    | 99          | 977.5             | 10 <i>sec</i> | (Ji et al., 2022a)            |
| MOFs   | Hg    | 97          | –                 | 2             | (Wu et al., 2021)             |
| MoS <sub>4</sub> -MOF                                  | Hg    | –           | 714.3             | –             | (Nozohour Yazdi et al., 2021) |
| Fe <sub>3</sub> O <sub>4</sub> – Cu-MOF (i-MOF)        | Pb    | 93          | 610               | –             | (Goyal et al., 2021)          |
| MIL-100 (Fe)   | Pb    | 99.35       | –                 | –             | (Zhang et al., 2021b)         |
| Zn(Bim)(OAc)   | Pb    | –           | 253.8             | 30            | (Xu et al., 2020)             |
| Zn(Bim)(OAc)   | Cu    | –           | 335.57            | 90            | (Xu et al., 2020)             |
| Fe-BTC/PDA   | Hg    | 99.8        | 1634              | –             | (Sun et al., 2018)            |
| UiO-66, UiO-67 MOFs                                    | Pb    | 95          | 366               | –             | (Morcos et al., 2021)         |
| Zr-MOF   | Hg    | 90          | 1080              | 10            | (Wang et al., 2020a)          |
| Zr-MOF   | Pb    | 90          | 510               | 90            | (Wang et al., 2020a)          |
| HKUST-1  | Pb    | –           | 819.28            | 60            | (Wang et al., 2021b)          |
| ZIF-8-EGCG   | Cu    | –           | 232.97            | –             | (Wen and Hu, 2021)            |
| FE-SEM. ZT-MOFs  | Au    | 94.5        | 333.34            | 480           | (Huang et al., 2020)          |
| UiO-66-NH <sub>2</sub>                                 | Hg    | –           | 327.88            | –             | (Feng et al., 2021b)          |
| Zr-based MOFs  | Cr    | –           | 338.98            | –             | (Chen et al., 2023)           |
| MIL-121  | Cu    | 99          | –                 | –             | (Ji et al., 2022b)            |
| MIL-121  | Pb    | 99          | –                 | –             | (Ji et al., 2022b)            |
| Fe-BTC/PDA   | Pb    | 99.8        | 394               | –             | (Sun et al., 2018)            |
| MOFs   | Pb    | –           | 537.634           | –             | (Zheng et al., 2021)          |
| MOFs   | Cr    | –           | 787.402           | –             | (Zheng et al., 2021)          |
| MOFs   | Hg    | –           | 269               | –             | (Rouhani and Morsali, 2018)   |
| MOFs   | Pb    | –           | 215               | –             | (Rouhani and Morsali, 2018)   |
| UiO-66-Cl  | Fe    | –           | 490               | –             | (Yuan et al., 2022b)          |
| UiO-66-S   | Fe    | –           | 285               | –             | (Yuan et al., 2022b)          |
| Fe <sub>3</sub> O <sub>4</sub> @ZIF-8                  | Cd    | 64          | –                 | –             | (Abdel-Magied et al., 2022)   |
| Fe <sub>3</sub> O <sub>4</sub> @ZIF-8                  | Pb    | 90          | –                 | –             | (Abdel-Magied et al., 2022)   |
| Fe <sub>3</sub> O <sub>4</sub> @UiO-66-NH <sub>2</sub> | Cd    | 85          | –                 | –             | (Abdel-Magied et al., 2022)   |
| Fe <sub>3</sub> O <sub>4</sub> @UiO-66-NH <sub>2</sub> | Pb    | 97          | –                 | –             | (Abdel-Magied et al., 2022)   |
| Fe <sub>3</sub> O <sub>4</sub> @ZIF-8                  | Cd    | 64          | –                 | –             | (Abdel-Magied et al., 2022)   |
| Fe <sub>3</sub> O <sub>4</sub> @ZIF-8                  | Pb    | 89          | –                 | –             | (Abdel-Magied et al., 2022)   |
| Fe <sub>3</sub> O <sub>4</sub> @UiO-66-NH <sub>2</sub> | Cd    | 85          | –                 | –             | (Abdel-Magied et al., 2022)   |
| Fe <sub>3</sub> O <sub>4</sub> @UiO-66-NH <sub>2</sub> | Pb    | 97          | –                 | –             | (Abdel-Magied et al., 2022)   |

and Pb) are soft acids, while  $\text{Ca}^{2+}$  and  $\text{Mg}^{2+}$  are hard acids (Fu and Huang, 2018; Jeyaseelan et al., 2021a). The presence of nitrogen groups of 2-methylimidazole ( $\text{Fe}_3\text{O}_4@\text{ZIF-8}$ ) prefers  $\text{Pb}^{2+}$  and  $\text{Cu}^{2+}$  over  $\text{Ca}^{2+}$  and  $\text{Mg}^{2+}$  (Fu and Huang, 2018). This makes  $\text{Fe}_3\text{O}_4@\text{ZIF-8}$  a highly selective for  $\text{Pb}^{2+}$  and  $\text{Cu}^{2+}$  in aqueous medium. Similarly, Jiang et al. (2021c) reported no effect of  $\text{Ca}^{2+}$ ,  $\text{Mg}^{2+}$ ,  $\text{SO}_4^{2-}$  and  $\text{Cl}^-$  on PTE adsorption by  $\text{Fe}_3\text{O}_4@\text{ZIF-8}$ . Likewise, Jeyaseelan et al. (2021a) showed M-BTC MOF selectivity for  $\text{F}^-$  removal over competing ions such as  $\text{CO}_3^{2-}$ ,  $\text{NO}_3^-$ ,  $\text{Cl}^-$ ,  $\text{SO}_4^{2-}$  and  $\text{PO}_4^{2-}$ .

Reports have demonstrated that the selectivity coefficients and distribution coefficients of competing ions for MOFs underline the selective removal of a PTE. Recently, Chen et al. (2023) revealed high selective adsorption of  $\text{Cr}^{6+}$  by Form-UiO-66- $\text{NH}_2$  compared to other PTEs. They reported that selectivity coefficient of Form-UiO-66- $\text{NH}_2$  for  $\text{Cr}^{6+}$  had severalfold higher values than competing PTEs. The selectivity coefficient values were about 45-times higher than Ni, 50-times higher than Pb, 56-times higher than Cu, 41-times higher than Cd and 58-times higher than  $\text{Cr}^{3+}$  (Chen et al., 2023). Authors revealed that Form-UiO-66- $\text{NH}_2$  possesses positive charge at pH 2 that could be a possible reason of high selectivity coefficient for  $\text{Cr}^{6+}$  than other PTEs. The positively-charged MOFs adsorbed negatively-charged  $\text{Cr}^{6+}$  but repelled positively-charged PTEs, thus making this adsorbent a highly selective adsorbent for  $\text{Cr}^{6+}$ .

Wastewaters usually contain more concentration of organic molecules than surface waters. Therefore, some recent studies also tested the effect of these competing organic molecules with the PTE adsorption capacity of MOFs in wastewaters. Sun et al. (2018) tested Fe-BTC/PDA potential to selectively remove Pb from wastewater sample containing high amount of organic molecules (up to 14 000 times that of  $\text{Pb}^{2+}$ ). The Fe-BTC/PDA reduced Pb level from 700 ppb to 2 ppb. The porous material showed about 70 % Pb removal in the first minute, 90 % in 60 min, and up to 99.8 % in 24 h (Sun et al., 2018).

The levels of competing cations and targeted PTE also affect the selectivity process (Wen and Hu, 2021). Despite the presence of 10-fold higher levels of anions, Dyes  $\subset$  MOF-80 was able to adsorb 83 mg/g of  $\text{Cr}_2\text{O}_7^{2-}$  from wastewater within 3 min. Similarly, Fe-BTC/PDA has shown an exceptional efficiency to adsorb high levels of Hg and Pb from natural water with unprecedented rate and selectivity. It was demonstrated that Fe-BTC/PDA decreased Pb contents in natural water (in the presence of competing ions) to drinkable levels in < 1 min. Mostly, the selective nature of an MOF for a PTE is developed by introducing extrinsic porosity to an MOF structure. Future research needs more focus on the synthesis and underlying mechanisms of PTE selectivity by MOFs under natural conditions having different types and compositions of competing ions.

**Table 8** Application of MOFs to remediate multi-metal(loid) and multi-pollutant contaminated wastewaters (recent data literature 2018–21).

| Materials                                 | Multi metal removal   | Reference                    |
|---|---|------------------------------|
| Multi-metal(loid) contaminated wastewater |   |                              |
| MOFs                                      | Cr (73 %), Pb (55 %), Zn (35 %)   | (Zheng et al., 2021)         |
| (MOF) ZIF-8                               | Pb (164–220 mg/g), Cd (92–161 mg/g)   | (Roy et al., 2021)           |
| Ag-Mg-MOF                                 | Pb (350 mg/g) > Cd (270 mg/g) > Cu (202 mg/g)   | (El-Hakam et al., 2021)      |
| UiO-66-EDA                                | Pb (243.90 mg/g) > Cd (217.39 mg/g) > Cu (208.33 mg/g)  | (Ahmadijokani et al., 2021)  |
| UiO-66-EDTA                               | Eu (195.2), Hg (371.6) and Pb (357.9)   | (Wu et al., 2019)            |
| UIO-67-EDTA                               | $\text{Cr}^{3+}$ (416.67), $\text{Hg}^{2+}$ (256.41) and $\text{Pb}^{2+}$ (312.15 mg/g)                                 | (Nie et al., 2021)           |
| Ag-Fe MOF                                 | Cd (265 mg/g) and Cu (213 mg/g)   | (Abo El-Yazeed et al., 2020) |
| UiO-66-GMA                                | Cu (90 %), Cd (82 %), Pb (79 %)   | (Gul Zaman et al., 2022)     |
| UiO-66-GMA                                | 85 % Cd and 76 % Cu   | (Gul Zaman et al., 2022)     |
| UiO-66-GMA                                | 91 % Cd and 89 % Pb   | (Gul Zaman et al., 2022)     |
| UiO-66-GMA                                | 82 % Cu and 76 % Pb   | (Gul Zaman et al., 2022)     |
| MOF-2 (Cd)                                | Pb (769.23 mg/g) and Cu (434.78 mg/g)   | (Ghaedi et al., 2018)        |
| Multi-pollutant contaminated wastewater   |   |                              |
| Zr-MFC-N                                  | Pb (102 mg/g) and methylene blue (128 mg/g)   | (Huang et al., 2018a)        |
| MOF@CNT                                   | $\text{Au}^{3+}$ (1832 mg/g) and $\text{Pd}^{2+}$ (1651 mg/g)   | (Zuhra et al., 2021)         |
| Zr-MOF                                    | Pb (100 mg/g), Cd (37 mg/g) and MB dye (169 mg/g)   | (Nimbalkar and Bhat, 2021)   |
| ZnO-NP@Zn-MOF-                            | Cu (106.2 mg/g) and tetracycline (137.1 mg/g)   | (Guo et al., 2021)           |
| UiO-66 MOF                                | 66.1 mg/g F-, 30 mg/g $\text{Cr}^{6+}$ , 485.4 mg/g diclofenac sodium, 110 mg/g methylene blue and 793.7 mg/g congo red | (Rego et al., 2021)          |
| CaFu MOF                                  | Cd (781.2 mg/g) and imidacloprid (467.23 mg/g)  | (Singh et al., 2021)         |
| V2O5@Ch/Cu-TMA                            | $\text{Cr}^{6+}$ by 92.43 %–96.95 % and LEVO drug by 91.99 %–97.20 %  | (Mahmoud et al., 2021)       |



### 6.3. Multi-metal removal by MOFs: Role of competing ions

Although majority of the studies primarily focused on single metal(loid) removal efficiency of MOFs, however, few studies also focused on multi-metal(loid) removal (Table 8) (El-Hakam et al., 2021; Roy et al., 2021). This scenario is more applied under natural conditions where waters, especially wastewaters are generally contaminated with > one metal (loid). Table 8 summarizes recent studies reporting multi-metal(loid)s or multi-pollutants removal by different types of MOFs. For example, El-Hakam et al. (2021) reported Ag-Mg-MOF-mediated multi-metal removal (Pb by 350 mg/g, Cd by 270 mg/g and Cu by 202 mg/g). Similarly, bare UiO-66 is capable to effectively adsorb  $\text{Cr}^{6+}$  (86 mg/g) and  $\text{As}^{5+}$  (303 mg/g) from water (Wang et al., 2015a; Noraee et al., 2019; Boix et al., 2020). However, after functionalization with thiourea groups, UiO-66 becomes capable of adsorbing multiple PTEs (mg/g) such as  $\text{Hg}^{2+}$  (769),  $\text{As}^{5+}$  (303),  $\text{Pb}^{2+}$  (232),  $\text{Cr}^{3+}$  (117) and  $\text{Cd}^{2+}$  (49) (Noraee et al., 2019; Boix et al., 2020). This shows the efficiency of some MOFs to remediate more than one metal(loid) from wastewaters.

The multi-metal removal efficiency of MOFs depends on post-synthetic functionalization (adding additional materials to their crystalline structure), which enhances binding strength for several PTEs. For example, adding ethylenediaminetetraacetic acid (EDTA), a ligand with high binding strength for various PTEs, to MOF crystalline structure can enhance multi-metal adsorption potential. Nie et al. (2021) incorporated EDTA to MOF (UIO-67) and synthesized multifunctional UIO-67-EDTA. This MOF-EDTA-based trap was highly efficient to remove multiple co-existing PTEs (Pb, Mn, Cr, Co, Ni, Cu, Hg, Zn, Bi, Ag, Sn, Cd) from waters. Yan et al. (2022) revealed that UiO-66-EDTMPA adsorbed 8.77 ( $\text{Pb}^{2+}$ ), 5.19 ( $\text{Cu}^{2+}$ ) and 5.63 ( $\text{Cd}^{2+}$ ) times-higher PTEs compared to raw UiO-66.

Likewise, Ahmadijokani et al. (2021) assessed UiO-66-EDA removal efficiency for single, binary, and ternary metal(loid) solutions of Cd, Pb, and Cu. Under single-metal(loid) solution, they reported UiO-66-EDA-mediated removal efficiency of 89 %, 95 %, and 80 %, respectively for Cd, Pb, and Cu. There was a significant decrease in removal efficiency of Cu (down to 50 % in binary and 44 % in ternary solutions) and Cd (56 % in binary and 51 % ternary solutions). However, there was a minor reduction of Pb removal efficiency in binary and ternary solutions (down to 90 % with Cd, 93 % with Cu, and 88 % with Cd and Cu). Hence, the removal efficiencies may vary differently for different metal(loid)s under multi-metal(loid) contaminated aqueous medium (Ghaedi et al., 2018; Abo El-Yazeed et al., 2020; Ahmadijokani et al., 2021). Yet, more studies are warranted for multi-metal(loid) removal by MOFs to better understand the associated effects, trends and mechanisms.

### 6.4. Regeneration potential of MOFs

One of the key features of recently-synthesized MOFs is their capacity of effective regeneration, which makes them highly suitable for industrial application. Several studies successfully regenerated and reused MOFs to remove PTEs for 3–5 cycles in adsorption processes (Table 6) (Ahmadijokani et al., 2021; Chen et al., 2021; Fu et al., 2021; Jeyaseelan et al., 2021a). During four cycles of adsorption/desorption, the  $\text{Au}^{3+}$

removal rate by ZT-MOFs decreased only from 94 to 87 % (Huang et al., 2020), thereby indicating good application for  $\text{Au}^{3+}$  remediation. More recently, Ji et al. (2021) showed extraordinary regeneration and removal potential of MIL-121 for Ni and Pb (>99 % for both PTEs) up to 10 consecutive cycles of adsorption–desorption.

Generally, the adsorption mechanisms of PTEs on MOFs determine the regeneration/desorption of MOFs, and thereby their recycling capacity. Some MOFs have high binding affinity for certain PTEs, therefore they have a strong binding interaction with PTE resulting in a limited regeneration potential (Ahmadijokani et al., 2021; Chen et al., 2021; Fu et al., 2021; Jeyaseelan et al., 2021a). In fact, due to strong PTE binding with MOFs, there is limited possibility of their desorption from active sites. Hence, the binding sites become unavailable for PTE adsorption and reuse.

The regeneration processes involve the activation by opening accessible pores and open metal sites for adsorption of PTEs and other pollutants/elements. The highly ideal MOF retain their specific chemical and structural characteristics after activation/regeneration. In order to improve regeneration potential of MOFs, recent studies have developed effective MOF structures containing high porosity, hydrophobicity, specific heteroatoms, coordinative unsaturated metal sites, and covalent functionalization. Under certain scenarios, where MOFs cannot be successfully regenerated, they are converted to any other useful product such as metal-nanoparticles and nanocomposites (Kumar et al., 2019).

## 7. Conclusions and perspectives

The recent literature data (2018–22) about water contamination by PTEs has revealed a grave threat to environmental sustainability and human health at a global scale. The use and release of PTEs has almost become invincible in modern industrial processes. Therefore, the advent of highly effective sorbents has become the need of the day and coming future. Accordingly, the continuous environmental monitoring and their effective and timely remediation are highly necessary and unavoidable.

The recent literature data also delineated metal–organic frameworks (MOFs) as highly effective and efficient adsorbents owing to their numerous intrinsic characteristics such as high porosity, surface area, specific cavity structure, selectivity, reusability, and structural stability. Based on literature data, it is proposed that post-synthetic functionalization can introduce several highly useful characteristics to MOFs making them highly effective, stable, selective, and reusable materials to sorb PTEs at industrial level. Overall, MOFs have a wide range of adsorption characteristics, mechanisms, and capacities for a variety of PTEs under varied conditions. This review will act as guidelines for future studies regarding MOF-mediated PTE removal from wastewaters.

Based on available literature data, recent trends and potential research gaps, the following future perspectives have been put-forth.

- Despite their useful characteristics and increased use in different applications, the future research needs to focus on the development of MOFs with exceptional selectivity, excellent adsorption capacity, high chemical stability, and enhanced regeneration potential. Moreover, the synthesis processes need to be highly cost-effective, easy, simple, and green.
- Owing to their highly useful intrinsic characteristics, MOFs have great potential to remediate different types of pollutants. However, there is a need to further enhance the transformation of research from laboratory-to-pilot scale.

- There exist different compositions of wastewater depending on the types of pollutants and competing ions. Hence, it remains a significant challenge to develop condition-specific MOFs such as for single-, binary-, ternary- and multi-pollutant contaminated conditions along with the occurrence of competing ions.
- Besides their high effectiveness for adsorption processes, there is a great need to monitor the possible environmental toxicology of synthesized MOFs for sustainable remediation.
- Nowadays, some companies (such as NuMat Technologies, BASF, MOFapps, ImmondoTech, framergy, MOF Technologies etc.) are mediating mass production of certain MOFs for their industrial applications, including ion doping in semiconductors, toxic gas adsorptions, and gas storages. To further facilitate the large-scale MOF synthesis, economic and green synthesis processes need further research.

### Declaration of Competing Interest

Authors declare no known competing financial interests.

### Acknowledgements

The authors are grateful to the support and fund by the Distinguished Scientist Fellowship Program (DSFP-2022), King Saud University, Riyadh, Saudi Arabia.

### Appendix A. Supplementary material

Supplementary data to this article can be found online at <https://doi.org/10.1016/j.arabjc.2022.104319>.

### References

- Abdelhamid, H.N., Georgouvelas, D., Edlund, U., Mathew, A.P., 2022. CelloZIFpaper: Cellulose-ZIF hybrid paper for heavy metal removal and electrochemical sensing. *Chem. Eng. J.* 446, 136614.
- Abdel-Magied, A.F., Abdelhamid, H.N., Ashour, R.M., Fu, L., Dowaidar, M., Xia, W., Forsberg, K., 2022. Magnetic metal-organic frameworks for efficient removal of cadmium(II), and lead (II) from aqueous solution. *J. Environ. Chem. Eng.* 10, 107467.
- Abo El-Yazeed, W.S., Abou El-Reash, Y.G., Elatwy, L.A., Ahmed, A.I., 2020. Novel bimetallic Ag-Fe MOF for exceptional Cd and Cu removal and 3,4-dihydropyrimidinone synthesis. *J. Taiwan Inst. Chem. Eng.* 114, 199–210.
- Ahmad, K., Ashfaq, M., Shah, S.S.A., Hussain, E., Naseem, H.A., Parveen, S., Ayub, A., 2021. Effect of metal atom in zeolitic imidazolate frameworks (ZIF-8 & 67) for removal of Pb<sup>2+</sup> & Hg<sup>2+</sup> from water. *Food Chem. Toxicol.* 149, 112008.
- Ahmadijokani, F., Tajahmadi, S., Bahi, A., Molavi, H., Rezakazemi, M., Ko, F., Aminabhavi, T.M., Arjmand, M., 2021. Ethylenediamine-functionalized Zr-based MOF for efficient removal of heavy metal ions from water. *Chemosphere* 264, 128466.
- Ahmed, I., Jhung, S.H., 2017. Applications of metal-organic frameworks in adsorption/separation processes via hydrogen bonding interactions. *Chem. Eng. J.* 310, 197–215.
- Ahmed, I., Lee, Y.-R., Yu, K., Bhattacharjee, S., Ahn, W.-S., 2019. Gd<sup>3+</sup> adsorption over carboxylic-and amino-group dual-functionalized UiO-66. *Ind. Eng. Chem. Res.* 58, 2324–2332.
- Aigbe, U.O., Osibote, O.A., 2021. Carbon derived nanomaterials for the sorption of heavy metals from aqueous solution: A review. *Environ. Nanotechnol. Monit. Manage.* 16, 100578.
- Aldakhil, F., Sirry, S., Alothman, Z.A., Ali, I., 2018. Lignocellulosic date stone for uranium (VI) uptake: Surface acidity, uptake capacity, kinetic and equilibrium. *J. Mol. Liq.* 269, 775–782.
- Ali, H., Khan, E., Ilahi, I., 2019. Environmental chemistry and ecotoxicology of hazardous heavy metals: environmental persistence, toxicity, and bioaccumulation. *J. Chem.* 2019.
- Aljaddua, H.I., Alhumaimess, M.S., Hassan, H.M.A., 2022. CaO nanoparticles incorporated metal organic framework (NH<sub>2</sub>-MIL-101) for Knoevenagel condensation reaction. *Arabian J. Chem.* 15, 103588.
- Alkas, T.R., Ediati, R., Ersam, T., Nawfa, R., Purnomo, A.S., 2022. Fabrication of metal-organic framework Universitas i Oslo-66 (UiO-66) and brown-rot fungus *Gloeophyllum trabeum* biocomposite (UiO-66@GT) and its application for reactive black 5 decolorization. *Arabian J. Chem.* 15, 104129.
- Alomar, T.S., AlMasoud, N., Sharma, G., ALOthman, Z.A., Naushad, M., 2021. Incorporation of trimetallic nanoparticles to the SiO<sub>2</sub> matrix for the removal of methylene blue dye from aqueous medium. *J. Mol. Liquids* 336.
- Alothman, Z.A., Bahkali, A.H., Khiyami, M.A., Alfadul, S.M., Wabaidur, S.M., Alam, M., Alfarhan, B.Z., 2020. Low cost biosorbents from fungi for heavy metals removal from wastewater. *Sep. Sci. Technol.* 55, 1766–1775.
- Alqadami, A.A., Naushad, M., ALOthman, Z.A., Alsuhybani, M., Algamdi, M., 2020b. Excellent adsorptive performance of a new nanocomposite for removal of toxic Pb (II) from aqueous environment: adsorption mechanism and modeling analysis. *J. Hazardous Mater.* 389.
- Alqadami, A.A., Khan, M.A., Siddiqui, M.R., Alothman, Z.A., 2018a. Development of citric anhydride anchored mesoporous MOF through post synthesis modification to sequester potentially toxic lead (II) from water. *Microporous Mesoporous Mater.* 261, 198–206.
- Alqadami, A.A., Naushad, M., Alothman, Z., Ahamad, T., 2018b. Adsorptive performance of MOF nanocomposite for methylene blue and malachite green dyes: kinetics, isotherm and mechanism. *J. Environ. Manage.* 223, 29–36.
- Alqadami, A.A., Khan, M.A., Siddiqui, M.R., Alothman, Z.A., Sumbul, S., 2020a. A facile approach to develop industrial waste encapsulated cryogenic alginate beads to sequester toxic bivalent heavy metals. *J. King Saud Univ.-Sci.* 32, 1444–1450.
- Al-Wasidi, A.S., Naglah, A.M., Saad, F.A., Abdelrahman, E.A., 2022. Modification of silica nanoparticles with 1-hydroxy-2-acetonaphthone as a novel composite for the efficient removal of Ni(II), Cu(II), Zn(II), and Hg(II) ions from aqueous media. *Arabian J. Chem.* 15, 104010.
- Ansarian, Z., Khataee, A., Arefi-Oskoui, S., Orooji, Y., Lin, H., 2022. Ultrasound-assisted catalytic activation of peroxydisulfate on Ti<sub>3</sub>GeC<sub>2</sub> MAX phase for efficient removal of hazardous pollutants. *Mater. Today Chem.* 24, 100818.
- Anwar, H., Shahid, M., Natasha, Niaz, N.K., Khalid, S., Tariq, T. Z., Ahmad, S., Nadeem, M., Abbas, G., 2021. Risk assessment of potentially toxic metal(loid)s in *Vigna radiata* L. under wastewater and freshwater irrigation. *Chemosphere* 265.
- AQUASTAT, 2022. Accessed: November, 11, 2021. <https://www.fao.org/aquastat/statistics/query/index.html?jsessionid=BBAB34E78DA1D73D1CE2FDC12A404BB9>.
- Batra, R., Chen, C., Evans, T.G., Walton, K.S., Ramprasad, R., 2020. Prediction of water stability of metal-organic frameworks using machine learning. *Nature Machine Intell.* 2, 704–710.
- Boix, G., Troyano, J., Garzón-Tovar, L., Camur, C., Bermejo, N., Yazdi, A., Piella, J., Bastus, N.G., Puentes, V.F., Imaz, I., MasPOCH, D., 2020. MOF-Beads Containing Inorganic Nanoparticles for the Simultaneous Removal of Multiple Heavy Metals from Water. *ACS Appl. Mater. Interfaces* 12, 10554–10562.
- Boretti, A., Rosa, L., 2019. Reassessing the projections of the world water development report. *npj Clean Water* 2, 1–6.
- Briffa, J., Sinagra, E., Blundell, R., 2020. Heavy metal pollution in the environment and their toxicological effects on humans. *Heliyon* 6, e04691.

- Burtch, N.C., Jasuja, H., Walton, K.S., 2014. Water stability and adsorption in metal-organic frameworks. *Chem. Rev.* 114, 10575–10612.
- Cai, G., Ma, X., Kassymova, M., Sun, K., Ding, M., Jiang, H.-L., 2021. Large-Scale Production of Hierarchically Porous Metal-Organic Frameworks by a Reflux-Assisted Post-Synthetic Ligand Substitution Strategy. *ACS Cent. Sci.* 7, 1434–1440.
- Cao, H., Xie, X., Wang, Y., Deng, Y., 2021. The interactive natural drivers of global geogenic arsenic contamination of groundwater. *J. Hydrol.* 597, 126214.
- Cao, Y., Zhang, H., Song, F., Huang, T., Ji, J., Zhong, Q., Chu, W., Xu, Q., 2018. UiO-66-NH<sub>2</sub>/GO Composite: Synthesis, Characterization and CO<sub>2</sub> Adsorption Performance. *Materials* 11, 589.
- Chen, W., Cai, Y., Lv, Z., Wang, X., Feng, J., Fang, M., Tan, X., 2021. Improvement of U (VI) removal by tuning magnetic metal organic frameworks with amine ligands. *J. Mol. Liq.* 334, 116495.
- Chen, P., Wang, Y., Zhuang, X., Liu, H., Liu, G., Lv, W., 2023. Selective removal of heavy metals by Zr-based MOFs in wastewater: New acid and amino functionalization strategy. *J. Environ. Sci.* 124, 268–280.
- Cheng, K., Wu, Y.-N., Zhang, B., Li, F., 2020. New insights into the removal of antimony from water using an iron-based metal-organic framework: Adsorption behaviors and mechanisms. *Colloids Surf., A* 602, 125054.
- Chñas-Rojas, L.E., Vivar-Vera, G., Cruz-Martínez, Y.F., Colohua, S.L., Rivera, J.M., Houbbron, E., 2022. Transition Metals-Based Metal-Organic Frameworks, Synthesis, and Environmental Applications. *Sorption - From Fundamentals to Applications*.
- Cui, H., Ye, Y., Liu, T., Allothman, Z.A., Alduhaish, O., Lin, R.-B., Chen, B., 2020. Isorecticular Microporous Metal-Organic Frameworks for Carbon Dioxide Capture. *Inorg. Chem.* 59, 17143–17148.
- Daradmare, S., Xia, M., Kim, J., Park, B.J., 2021. Metal-organic frameworks/alginate composite beads as effective adsorbents for the removal of hexavalent chromium from aqueous solution. *Chemosphere* 270, 129487.
- Devic, T., Serre, C., 2014. High valence 3p and transition metal based MOFs. *Chem. Soc. Rev.* 43, 6097–6115.
- Ding, M., Cai, X., Jiang, H.-L., 2019. Improving MOF stability: approaches and applications. *Chem. Sci.* 10, 10209–10230.
- Efome, J.E., Rana, D., Matsuura, T., Lan, C.Q., 2018. Metal-organic frameworks supported on nanofibers to remove heavy metals. *J. Mater. Chem. A* 6, 4550–4555.
- El-Hakam, S.A., Ibrahim, A.A., Elatwy, L.A., El-Yazeed, W.S.A., Salama, R.S., El-Reash, Y.G.A., Ahmed, A.I., 2021. Greener route for the removal of toxic heavy metals and synthesis of 14-aryl-14H dibenzo[a, j] xanthene using a novel and efficient Ag-Mg bimetallic MOF as a recyclable heterogeneous nanocatalyst. *J. Taiwan Inst. Chem. Eng.* 122, 176–189.
- Esrafil, L., Firuzabadi, F.D., Morsali, A., Hu, M.-L., 2021. Reuse of pre-designed dual-functional metal organic frameworks (DF-MOFs) after heavy metal removal. *J. Hazard. Mater.* 403, 123696.
- Feng, L., Zeng, T., Hou, H., 2021a. Post-functionalized metal-organic framework for effective and selective removal of Hg (II) in aqueous media. *Microporous Mesoporous Mater.* 328, 111479.
- Feng, L., Zeng, T., Hou, H., 2021b. Post-functionalized metal-organic framework for effective and selective removal of Hg(II) in aqueous media. *Microporous Mesoporous Mater.* 328, 111479.
- Feng, M., Zhang, P., Zhou, H.-C., Sharma, V.K., 2018. Water-stable metal-organic frameworks for aqueous removal of heavy metals and radionuclides: A review. *Chemosphere* 209, 783–800.
- Figueira, F., Mendes, R.F., Domingues, E.M., Barbosa, P., Figueiredo, F., Paz, F.A., Rocha, J., 2020. Easy Processing of Metal-Organic Frameworks into Pellets and Membranes. *Appl. Sci.* 10, 798.
- Forsyth, C., Taras, T., Johnson, A., Zagari, J., Collado, C., Hoffmann, M.M., Reed, C.R., 2020. Microwave assisted surfactant-thermal synthesis of metal-organic framework materials. *Appl. Sci.* 10, 4563.
- Fu, W., Huang, Z.G., 2018. One-Pot Synthesis of a Two-Dimensional Porous Fe<sub>3</sub>O<sub>4</sub>/Poly(C<sub>3</sub>N<sub>3</sub>S<sub>3</sub>) Network Nanocomposite for the Selective Removal of Pb(II) and Hg(II) from Synthetic Wastewater. *ACS Sustainable Chem. Eng.*
- Fu, Q., Lou, J., Peng, L., Zhang, R., Zhou, S., Wu, P., Yan, W., Mo, C., Luo, J., 2021. Iron based metal organic framework for efficient removal of Pb<sup>2+</sup> from wastewater. *J. Solid State Chem.* 300, 122188.
- Fu, L., Wang, S., Lin, G., Zhang, L., Liu, Q., Fang, J., Wei, C., Liu, G., 2019. Post-functionalization of UiO-66-NH<sub>2</sub> by 2, 5-Dimercapto-1, 3, 4-thiadiazole for the high efficient removal of Hg (II) in water. *J. Hazard. Mater.* 368, 42–51.
- Fuentes-Fernandez, E., Jensen, S., Tan, K., Zuluaga, S., Wang, H., Li, J., Thonhauser, T., Chabal, Y.J., 2018. Controlling Chemical Reactions in Confined Environments: Water Dissociation in MOF-74. *Appl. Sci.* 8, 270.
- Gaikwad, S., Cheedarala, R.K., Gaikwad, R., Kim, S., Han, S., 2021. Controllable Synthesis of 1, 3, 5-tris (1H-benzo [d] imidazole-2-yl) Benzene-Based MOFs. *Appl. Sci.* 11, 9856.
- Gao, M., Liu, G., Gao, Y., Chen, G., Huang, X., Xu, X., Wang, J., Yang, X., Xu, D., 2021a. Recent advances in metal-organic frameworks/membranes for adsorption and removal of metal ions. *TrAC, Trends Anal. Chem.* 137, 116226.
- Gao, T., Tang, H.-J., Zhang, S.-Y., Cao, J.-W., Wu, Y.-N., Chen, J., Wang, Y., Chen, K.-J., 2021b. Mechanochemical synthesis of three-component metal-organic frameworks for large scale production. *J. Solid State Chem.* 303, 122547.
- Ghaedi, M., 2021. Adsorption: Fundamental Processes and Applications. Elsevier.
- Ghaedi, A.M., Panahimehr, M., Nejad, A.R.S., Hosseini, S.J., Vafaei, A., Baneshi, M.M., 2018. Factorial experimental design for the optimization of highly selective adsorption removal of lead and copper ions using metal organic framework MOF-2 (Cd). *J. Mol. Liq.* 272, 15–26.
- Ghorbani-Choghamarani, A., Taherinia, Z., Mohammadi, M., 2021. Facile synthesis of Fe<sub>3</sub>O<sub>4</sub>@GlcA@Ni-MOF composites as environmentally green catalyst in organic reactions. *Environ. Technol. Innovation*, 102050.
- Ghosh, A., Das, G., 2020. Green synthesis of a novel water-stable Sn (ii)-TMA metal-organic framework (MOF): an efficient adsorbent for fluoride in aqueous medium in a wide pH range. *New J. Chem.* 44, 1354–1361.
- Goyal, P., Tiwary, C.S., Misra, S.K., 2021. Ion exchange based approach for rapid and selective Pb(II) removal using iron oxide decorated metal organic framework hybrid. *J. Environ. Manage.* 277, 111469.
- Gul, S., Ahmad, Z., Asma, M., Ahmad, M., Rehan, K., Munir, M., Bazmi, A.A., Ali, H.M., Mazroua, Y., Salem, M.A., Akhtar, M.S., Khan, M.S., Chuah, L.F., Asif, S., 2022. Effective adsorption of cadmium and lead using SO<sub>3</sub>H-functionalized Zr-MOFs in aqueous medium. *Chemosphere* 307, 135633.
- Gul Zaman, H., Baloo, L., Rahman Kutty, S., Altaf, M., 2022. Post Synthetic Modification of NH<sub>2</sub>-(Zr-MOF) via Rapid Microwave-Promoted Synthesis for Effective Adsorption of Pb(II) and Cd(II). *Arabian J. Chem.*, 104122
- Guo, Z., Yang, F., Yang, R., Sun, L., Li, Y., Xu, J., 2021. Preparation of novel ZnO-NP@Zn-MOF-74 composites for simultaneous removal of copper and tetracycline from aqueous solution. *Sep. Purif. Technol.* 274, 118949.
- Habila, M., Allothman, Z., Yilmaz, E., Alabdulkarem, E., Soylok, M., 2019. A new amine based microextraction of lead (II) in real water samples using flame atomic absorption spectrometry. *Microchem. J.* 148, 214–219.
- Haftan, F., Motakef-Kazemi, N., 2021. The sorbent based on MOF-5 and its polyurethane nanocomposite for copper adsorption from aqueous solution. *Nanomed. Res. J.* 6, 287–295.
- Han, Y., Yang, H., Guo, X., 2020. Synthesis methods and crystallization of MOFs. *Synthesis Methods and Crystallization*. IntechOpen.

- Hasankola, Z.S., Rahimi, R., Safarifard, V., 2019. Rapid and efficient ultrasonic-assisted removal of lead (II) in water using two copper- and zinc-based metal-organic frameworks. *Inorg. Chem. Commun.* 107, 107474.
- Hasankola, Z.S., Rahimi, R., Shayegan, H., Moradi, E., Safarifard, V., 2020. Removal of Hg<sup>2+</sup> heavy metal ion using a highly stable mesoporous porphyrinic zirconium metal-organic framework. *Inorg. Chim. Acta* 501, 119264.
- Hou, X., Wang, J., Mousavi, B., Klomkliang, N., Chaemchuen, S., 2022. Strategies for induced defects in metal-organic frameworks for enhancing adsorption and catalytic performance. *Dalton Trans.* 51, 8133–8159.
- Hu, X., Alsaikhan, F., Majdi, H.S., Bokov, D.O., Mohamed, A., Sadeghi, A., 2022b. Predictive modeling and computational machine learning simulation of adsorption separation using advanced nanocomposite materials. *Arabian J. Chem.* 15, 104062.
- Hu, S.-Z., Huang, T., Zhang, N., Lei, Y.-Z., Wang, Y., 2022a. Chitosan-assisted MOFs dispersion via covalent bonding interaction toward highly efficient removal of heavy metal ions from wastewater. *Carbohydr. Polym.* 277, 118809.
- Hu, Y., Yang, H., Wang, R., Duan, M., 2021. Fabricating Ag@MOF-5 nanoplates by the template of MOF-5 and evaluating its antibacterial activity. *Colloids Surf., A* 626, 127093.
- Hu, Z., Zhao, D., 2017. Metal-organic frameworks with Lewis acidity: synthesis, characterization, and catalytic applications. *CrystEngComm* 19, 4066–4081.
- Huang, L., He, M., Chen, B., Hu, B., 2018a. Magnetic Zr-MOFs nanocomposites for rapid removal of heavy metal ions and dyes from water. *Chemosphere* 199, 435–444.
- Huang, L., Yang, Z., Alhassan, S.I., Luo, Z., Song, B., Jin, L., Zhao, Y., Wang, H., 2021. Highly efficient fluoride removal from water using 2D metal-organic frameworks MIL-53 (Al) with rich Al and O adsorptive centers. *Environ. Sci. Ecotechnol.* 8, 100123.
- Huang, Y., Zeng, X., Guo, L., Lan, J., Zhang, L., Cao, D., 2018b. Heavy metal ion removal of wastewater by zeolite-imidazolate frameworks. *Sep. Purif. Technol.* 194, 462–469.
- Huang, Z., Zhao, M., Wang, S., Dai, L., Zhang, L., Wang, C., 2020. Selective recovery of gold ions in aqueous solutions by a novel trithiocyanuric-Zr based MOFs adsorbent. *J. Mol. Liq.* 298, 112090.
- Ibrahim, A.O., Adegoke, K.A., Adegoke, R.O., AbdulWahab, Y.A., Oyelami, V.B., Adesina, M.O., 2021. Adsorptive removal of different pollutants using metal-organic framework adsorbents. *J. Mol. Liq.* 115593
- Jeyaseelan, A., Albaqami, M.D., Viswanathan, N., 2021a. Facile design of metal ion fabricated benzene-1,3,5-tricarboxylic acid based metal organic frameworks for defluoridation of water. *J. Environ. Chem. Eng.* 9, 104995.
- Jeyaseelan, A., Albaqami, M.D., Viswanathan, N., 2021b. Facile design of metal ion fabricated benzene-1, 3, 5-tricarboxylic acid based metal organic frameworks for defluoridation of water. *J. Environ. Chem. Eng.* 9, 104995.
- Jeyaseelan, A., Naushad, M., Ahamad, T., Viswanathan, N., 2021c. Design and development of amine functionalized iron based metal organic frameworks for selective fluoride removal from water environment. *J. Environ. Chem. Eng.* 9, 104563.
- Ji, C., Xu, M., Yu, H., Lv, L., Zhang, W., 2021. Mechanistic insight into selective adsorption and easy regeneration of carboxyl-functionalized MOFs towards heavy metals. *J. Hazard. Mater.* 127684
- Ji, C., Ren, Y., Yu, H., Hua, M., Lv, L., Zhang, W., 2022a. Highly efficient and selective Hg(II) removal from water by thiol-functionalized MOF-808: Kinetic and mechanism study. *Chem. Eng. J.* 430, 132960.
- Ji, C., Xu, M., Yu, H., Lv, L., Zhang, W., 2022b. Mechanistic insight into selective adsorption and easy regeneration of carboxyl-functionalized MOFs towards heavy metals. *J. Hazard. Mater.* 424, 127684.
- Jiang, X., Su, S., Rao, J., Li, S., Lei, T., Bai, H., Wang, S., Yang, X., 2021b. Magnetic metal-organic framework (Fe<sub>3</sub>O<sub>4</sub>@ZIF-8) core-shell composite for the efficient removal of Pb (II) and Cu (II) from water. *J. Environ. Chem. Eng.* 9, 105959.
- Jiang, X., Su, S., Rao, J., Li, S., Lei, T., Bai, H., Wang, S., Yang, X., 2021c. Magnetic metal-organic framework (Fe<sub>3</sub>O<sub>4</sub>@ZIF-8) core-shell composite for the efficient removal of Pb(II) and Cu(II) from water. *J. Environ. Chem. Eng.* 9, 105959.
- Jiang, C., Zhao, Q., Zheng, L., Chen, X., Li, C., Ren, M., 2021a. Distribution, source and health risk assessment based on the Monte Carlo method of heavy metals in shallow groundwater in an area affected by mining activities, China. *Ecotoxicol. Environ. Saf.* 224, 112679.
- Karmakar, S., Bhattacharjee, S., De, S., 2018. Aluminium fumarate metal organic framework incorporated polyacrylonitrile hollow fiber membranes: Spinning, characterization and application in fluoride removal from groundwater. *Chem. Eng. J.* 334, 41–53.
- Kaur, R., Wani, S., Singh, A., Lal, K., 2012. Wastewater production, treatment and use in India. National Report Presented at the 2nd Regional Workshop on Safe Use of Wastewater in Agriculture.
- Ke, F., Peng, C., Zhang, T., Zhang, M., Zhou, C., Cai, H., Zhu, J., Wan, X., 2018. Fumarate-based metal-organic frameworks as a new platform for highly selective removal of fluoride from brick tea. *Sci. Rep.* 8, 939.
- Keshavarz, F., Kavun, V., van der Veen, M.A., Repo, E., Barbiellini, B., 2022. Molecular-level understanding of highly selective heavy rare earth element uptake by organophosphorus modified MIL-101 (Cr). *Chem. Eng. J.* 440, 135905.
- Khalil, M., Shehata, M.M., Ghazy, O., Waly, S.A., Ali, Z.I., 2022. Synthesis, characterization and  $\gamma$ -rays irradiation of cobalt-based metal-organic framework for adsorption of Ce(III) and Eu(III) from aqueous solution. *Radiat. Phys. Chem.* 190, 109811.
- Kim, Y., Kim, K., Eom, H.H., Su, X., Lee, J.W., 2021. Electrochemically-assisted removal of cadmium ions by redox active Cu-based metal-organic framework. *Chem. Eng. J.* 421, 129765.
- Kobieliska, P.A., Howarth, A.J., Farha, O.K., Nayak, S., 2018. Metal-organic frameworks for heavy metal removal from water. *Coord. Chem. Rev.* 358, 92–107.
- Kumar, P., Anand, B., Tsang, Y.F., Kim, K.-H., Khullar, S., Wang, B., 2019. Regeneration, degradation, and toxicity effect of MOFs: Opportunities and challenges. *Environ. Res.* 176, 108488.
- Kumar, A., Cabral-Pinto, M., Kumar, M., Dinis, P.A., 2020. Estimation of risk to the eco-environment and human health of using heavy metals in the Uttarakhand Himalaya, India. *Appl. Sci.* 10, 7078.
- Lei, C., Gao, J., Ren, W., Xie, Y., Abdalkarim, S.Y.H., Wang, S., Ni, Q., Yao, J., 2019. Fabrication of metal-organic frameworks@cellulose aerogels composite materials for removal of heavy metal ions in water. *Carbohydr. Polym.* 205, 35–41.
- Leventeli, Y., Yalcin, F., Kilic, M., 2019. An investigation about heavy metal pollution of Duden and Goksu Streams (Antalya, Turkey). *Appl. Ecol. Environ. Res.* 17, 2423–2436.
- Li, Y., Huang, H., Xu, Z., Ma, H., Guo, Y., 2020b. Mechanism study on manganese(II) removal from acid mine wastewater using red mud and its application to a lab-scale column. *J. Cleaner Prod.* 253, 119955.
- Li, J., Liao, L., Jia, Y., Tian, T., Gao, S., Zhang, C., Shen, W., Wang, Z., 2022b. Magnetic Fe<sub>3</sub>O<sub>4</sub>/ZIF-8 optimization by Box-Behnken design and its Cd(II)-adsorption properties and mechanism. *Arabian J. Chem.* 15, 104119.
- Li, D., Tian, X., Wang, Z., Guan, Z., Li, X., Qiao, H., Ke, H., Luo, L., Wei, Q., 2020a. Multifunctional adsorbent based on metal-organic framework modified bacterial cellulose/chitosan composite aerogel for high efficient removal of heavy metal ion and organic pollutant. *Chem. Eng. J.* 383, 123127.
- Li, J.-H., Wang, Y.-S., Chen, Y.-C., Kung, C.-W., 2019. Metal-organic frameworks toward electrocatalytic applications. *Appl. Sci.* 9, 2427.

- Li, Z., Wang, L., Qin, L., Lai, C., Wang, Z., Zhou, M., Xiao, L., Liu, S., Zhang, M., 2021. Recent advances in the application of water-stable metal-organic frameworks: Adsorption and photocatalytic reduction of heavy metal in water. *Chemosphere*, 131432.
- Li, C., Wang, H., Liao, X., Xiao, R., Liu, K., Bai, J., Li, B., He, Q., 2022a. Heavy metal pollution in coastal wetlands: A systematic review of studies globally over the past three decades. *J. Hazard. Mater.* 424, 127312.
- Li, D., Xu, F., 2021. Removal of Cu (II) from aqueous solutions using ZIF-8@GO composites. *J. Solid State Chem.* 302, 122406.
- Liu, X., Shan, Y., Zhang, S., Kong, Q., Pang, H., 2022. Application of metal organic framework in wastewater treatment. *Green Energy Environ.*
- Liu, J., Wang, J., Xiao, T., Lippold, H., Luo, X., Yin, M., Ren, J., Chen, Y., Linghu, W., 2018. Geochemical dispersal of thallium and accompanying metals in sediment profiles from a smelter-impacted area in South China. *Appl. Geochem.* 88, 239–246.
- Liu, X., Wang, X., Kapteijn, F., 2020. Water and Metal-Organic Frameworks: From Interaction toward Utilization. *Chem. Rev.* 120, 8303–8377.
- Long, Z., Huang, Y., Zhang, W., Shi, Z., Yu, D., Chen, Y., Liu, C., Wang, R., 2021. Effect of different industrial activities on soil heavy metal pollution, ecological risk, and health risk. *Environ. Monit. Assess.* 193, 20.
- Ma, Q., Zhang, T., Wang, B., 2022. Shaping of metal-organic frameworks, a critical step toward industrial applications. *Matter* 5, 1070–1091.
- Mahmoodi, N.M., Taghizadeh, M., Taghizadeh, A., Abdi, J., Hayati, B., Shekarchi, A.A., 2019. Bio-based magnetic metal-organic framework nanocomposite: Ultrasound-assisted synthesis and pollutant (heavy metal and dye) removal from aqueous media. *Appl. Surf. Sci.* 480, 288–299.
- Mahmoud, M.E., Amira, M.F., Azab, M.M.H.M., Abdelfattah, A. M., 2021. Effective removal of levofloxacin drug and Cr(VI) from water by a composed nanobiosorbent of vanadium pentoxide@chitosan@MOFs. *Int. J. Biol. Macromol.* 188, 879–891.
- Mallakpour, S., Nikkhoo, E., Hussain, C.M., 2022. Application of MOF materials as drug delivery systems for cancer therapy and dermal treatment. *Coord. Chem. Rev.* 451, 214262.
- Mansouri, M., Sadeghian, S., Mansouri, G., Setareshenas, N., 2021. Enhanced photocatalytic performance of UiO-66-NH<sub>2</sub>/TiO<sub>2</sub> composite for dye degradation. *Environ. Sci. Pollut. Res.* 28, 25552–25565.
- Miao, S., Guo, J., Deng, Z., Yu, J., Dai, Y., 2022. Adsorption and reduction of Cr(VI) in water by iron-based metal-organic frameworks (Fe-MOFs) composite electrospun nanofibrous membranes. *J. Cleaner Prod.* 370, 133566.
- Mohan, B., Kumar, S., Virender, Kumar, A., Kumar, K., Modi, K., Jiao, T., Chen, Q., 2022. Analogize of metal-organic frameworks (MOFs) adsorbents functional sites for Hg<sup>2+</sup> ions removal. *Separat. Purif. Technol.* 297.
- Molavi, H., Eskandari, A., Shojaei, A., Mousavi, S.A., 2018. Enhancing CO<sub>2</sub>/N<sub>2</sub> adsorption selectivity via post-synthetic modification of NH<sub>2</sub>-UiO-66(Zr). *Microporous Mesoporous Mater.* 257, 193–201.
- Morcos, G.S., Ibrahim, A.A., El-Sayed, M.M.H., El-Shall, M.S., 2021. High performance functionalized UiO metal organic frameworks for the efficient and selective adsorption of Pb (II) ions in concentrated multi-ion systems. *J. Environ. Chem. Eng.* 9, 105191.
- Natasha, Shahid, M., Khalid, S., Niazi, N.K., Murtaza, B., Ahmad, N., Farooq, A., Zakir, A., Imran, M., Abbas, G., 2021. Health risks of arsenic buildup in soil and food crops after wastewater irrigation. *Sci. Total Environ.* 772.
- Natasha, Shahid, M., Khalid, S., Murtaza, B., Anwar, H., Shah, A. H., Sardar, A., Shabbir, Z., Niazi, N.K., 2020. A critical analysis of wastewater use in agriculture and associated health risks in Pakistan. *Environmental geochemistry and health.*
- Naushad, M., Ahamad, T., AlOthman, Z.A., Ala'a, H., 2019. Green and eco-friendly nanocomposite for the removal of toxic Hg (II) metal ion from aqueous environment: adsorption kinetics & isotherm modelling. *J. Mol. Liq.* 279, 1–8.
- Naushad, M., AlOthman, Z.A., 2015. Separation of toxic Pb<sup>2+</sup> metal from aqueous solution using strongly acidic cation-exchange resin: analytical applications for the removal of metal ions from pharmaceutical formulation. *Desalin. Water Treat.* 53, 2158–2166.
- Niazi, N.K., Bibi, I., Shahid, M., Ok, Y.S., Burton, E.D., Wang, H., Shaheen, S.M., Rinklebe, J., Lüttge, A., 2018. Arsenic removal by perilla leaf biochar in aqueous solutions and groundwater: An integrated spectroscopic and microscopic examination. *Environ. Pollut.* 232, 31–41.
- Nie, R., Yang, C., Zhang, J., Dong, K., Zhao, G., 2021. Removal of multiple metal ions from wastewater by a multifunctional metal-organic-framework based trap. *Water Sci. Technol. : A J. Int. Assoc. Water Pollut. Res.* 84, 1594–1607.
- Nimbalkar, M.N., Bhat, B.R., 2021. Simultaneous adsorption of methylene blue and heavy metals from water using Zr-MOF having free carboxylic group. *J. Environ. Chem. Eng.* 9, 106216.
- Noraee, Z., Jafari, A., Ghaderpoori, M., Kamarehie, B., Ghaderpoory, A., 2019. Use of metal-organic framework to remove chromium (VI) from aqueous solutions. *J. Environ. Health Sci. Eng.* 17, 701–709.
- Nozohour Yazdi, M., Dadfarnia, S., Haji Shabani, A.M., 2021. Synthesis of stable S- functionalized metal-organic framework using MoS<sub>4</sub><sup>2-</sup> and its application for selective and efficient removal of toxic heavy metal ions in wastewater treatment. *J. Environ. Chem. Eng.* 9, 104696.
- Nqombolo, A., Munonde, T.S., Makhetha, T.A., Moutloali, R.M., Nomngongo, P.N., 2021. Cobalt/zinc based metal organic frameworks as an effective adsorbent for improved removal of As (V) and Cr (VI) in a wide pH range. *J. Mater. Res. Technol.* 12, 1845–1855.
- Obasi, P., Akudinobi, B., 2019. Heavy metals occurrence, assessment and distribution in water resources of the lead–zinc mining areas of Abakaliki, Southeastern Nigeria. *Int. J. Environ. Sci. Technol.* 16, 8617–8638.
- Omer, A.M., Dey, R., Eltaweil, A.S., Abd El-Monaem, E.M., Ziora, Z.M., 2022. Insights into recent advances of chitosan-based adsorbents for sustainable removal of heavy metals and anions. *Arabian J. Chem.* 15, 103543.
- Orooji, Y., Ghanbari, M., Amiri, O., Salavati-Niasari, M., 2020a. Facile fabrication of silver iodide/graphitic carbon nitride nanocomposites by notable photo-catalytic performance through sunlight and antimicrobial activity. *J. Hazard. Mater.* 389, 122079.
- Orooji, Y., Mohassel, R., Amiri, O., Sobhani, A., Salavati-Niasari, M., 2020b. Gd<sub>2</sub>ZnMnO<sub>6</sub>/ZnO nanocomposites: Green sol-gel auto-combustion synthesis, characterization and photocatalytic degradation of different dye pollutants in water. *J. Alloy. Compd.* 835, 155240.
- Orooji, Y., Akbari, R., Nezafat, Z., Nasrollahzadeh, M., Kamali, T. A., 2021a. Recent signs of progress in polymer-supported silver complexes/nanoparticles for remediation of environmental pollutants. *J. Mol. Liq.* 329, 115583.
- Orooji, Y., Tanhaei, B., Ayati, A., Tabrizi, S.H., Alizadeh, M., Bamoharram, F.F., Karimi, F., Salmanpour, S., Rouhi, J., Afshar, S., Sillanpää, M., Darabi, R., Karimi-Maleh, H., 2021b. Heterogeneous UV-Switchable Au nanoparticles decorated tungstophosphoric acid/TiO<sub>2</sub> for efficient photocatalytic degradation process. *Chemosphere* 281, 130795.
- Ouyang, B., Ouyang, P., Shi, M., Maimaiti, T., Li, Q., Lan, S., Luo, J., Wu, X., Yang, S.-T., 2021. Low toxicity of metal-organic framework MOF-199 to bacteria *Escherichia coli* and *Staphylococcus aureus*. *J. Hazard. Mater. Adv.* 1, 100002.
- Ouyang, B., Liu, F., Liang, C., Zhang, J., Hu, R., Yuan, H., Hai, R., Yuan, Y., Wu, X., Yang, S.-T., 2022. Toxicity and activity

- inhibition of metal-organic framework MOF-199 to nitrogen-fixing bacterium *Azotobacter vinelandii*. *Sci. Total Environ.* 813, 151912.
- Peng, Y., Huang, H., Zhang, Y., Kang, C., Chen, S., Song, L., Liu, D., Zhong, C., 2018. A versatile MOF-based trap for heavy metal ion capture and dispersion. *Nat. Commun.* 9, 1–9.
- Pillai, P., Dharaskar, S., Sasikumar, S., Khalid, M., 2019. Zeolitic imidazolate framework-8 nanoparticle: a promising adsorbent for effective fluoride removal from aqueous solution. *Appl. Water Sci.* 9, 150.
- Quyen, V.T., Pham, T.-H., Kim, J., Thanh, D.M., Thang, P.Q., Van Le, Q., Jung, S.H., Kim, T., 2021. Biosorbent derived from coffee husk for efficient removal of toxic heavy metals from wastewater. *Chemosphere* 284.
- Rani, S., Sharma, B., Kapoor, S., Malhotra, R., Varma, R.S., Dilbaghi, N., 2019. Construction of silver quantum dot immobilized Zn-MOF-8 composite for electrochemical sensing of 2, 4-dinitrotoluene. *Appl. Sci.* 9, 4952.
- Raptopoulou, C.P., 2021. Metal-Organic Frameworks: Synthetic Methods and Potential Applications. *Materials (Basel)* 14.
- Rego, R.M., Sriram, G., Ajeya, K.V., Jung, H.-Y., Kurkuri, M.D., Kigga, M., 2021. Cerium based UiO-66 MOF as a multipollutant adsorbent for universal water purification. *J. Hazard. Mater.* 416, 125941.
- Roudbari, R., Keramati, N., Ghorbani, M., 2021. Porous nanocomposite based on metal-organic framework: Antibacterial activity and efficient removal of Ni (II) heavy metal ion. *J. Mol. Liq.* 322, 114524.
- Rouhani, F., Morsali, A., 2018. Fast and Selective Heavy Metal Removal by a Novel Metal-Organic Framework Designed with In-Situ Ligand Building Block Fabrication Bearing Free Nitrogen. *Chem. – A Eur. J.* 24, 5529–5537.
- Roy, D., Neogi, S., De, S., 2021. Adsorptive removal of heavy metals from battery industry effluent using MOF incorporated polymeric beads: A combined experimental and modeling approach. *J. Hazard. Mater.* 403, 123624.
- Ru, J., Wang, X., Wang, F., Cui, X., Du, X., Lu, X., 2021. UiO series of metal-organic frameworks composites as advanced sorbents for the removal of heavy metal ions: Synthesis, applications and adsorption mechanism. *Ecotoxicol. Environ. Saf.* 208, 111577.
- Ryu, U., Jee, S., Rao, P.C., Shin, J., Ko, C., Yoon, M., Park, K.S., Choi, K.M., 2021. Recent advances in process engineering and upcoming applications of metal-organic frameworks. *Coord. Chem. Rev.* 426, 213544.
- Schernikau, M., Sablowski, J., Gonzalez Martinez, I.G., Unz, S., Kaskel, S., Mikhaилоva, D., 2021. Preparation and Application of ZIF-8 Thin Layers. *Appl. Sci.* 11, 4041.
- Shabbir, Z., Sardar, A., Shabbir, A., Abbas, G., Shamshad, S., Khalid, S., Murtaza, G., Dumat, C., Shahid, M., 2020a. Copper uptake, essentiality, toxicity, detoxification and risk assessment in soil-plant environment. *Chemosphere* 259, 127436.
- Shabbir, Z., Shahid, M., Khalid, S., Khalid, S., Imran, M., Qureshi, M.I., Niazi, N.K., 2020b. Use of agricultural bio-wastes to remove arsenic from contaminated water. *Environ. Geochem. Health*, 1–10.
- Shahid, M., 2021. Effect of soil amendments on trace element-mediated oxidative stress in plants: Meta-analysis and mechanistic interpretations. *J. Hazard. Mater.* 407, 124881.
- Shahid, M., Pinelli, E., Pourrut, B., Dumat, C., 2014a. Effect of organic ligands on lead-induced oxidative damage and enhanced antioxidant defense in the leaves of *Vicia faba* plants. *J. Geochem. Explor.* 144, 282–289.
- Shahid, M., Pourrut, B., Dumat, C., Nadeem, M., Aslam, M., Pinelli, E., 2014b. Heavy-metal-induced reactive oxygen species: phytotoxicity and physicochemical changes in plants. *Rev. Environ. Contam. Toxicol.* 232, 1–44.
- Shahid, M., Khalid, M., Dumat, C., Khalid, S., Niazi, N.K., Imran, M., Bibi, I., Ahmad, I., Hammad, H.M., Tabassum, R.A., 2018a. Arsenic Level and Risk Assessment of Groundwater in Vehari, Punjab Province, Pakistan. *Exposure Health* 10, 229–239.
- Shahid, M., Niazi, N.K., Dumat, C., Naidu, R., Khalid, S., Rahman, M.M., Bibi, I., 2018b. A meta-analysis of the distribution, sources and health risks of arsenic-contaminated groundwater in Pakistan. *Environ. Pollut.* 242, 307–319.
- Shahid, M., Khalid, S., Niazi, N.K., Murtaza, B., Ahmad, N., Farooq, A., Zakir, A., Imran, M., Abbas, G., 2021. Health risks of arsenic buildup in soil and food crops after wastewater irrigation. *Sci. Total Environ.* 772, 145266.
- Shaji, E., Santosh, M., Sarath, K.V., Prakash, P., Deepchand, V., Divya, B.V., 2021. Arsenic contamination of groundwater: A global synopsis with focus on the Indian Peninsula. *Geosci. Front.* 12, 101079.
- Shamim, M.A., Zia, H., Zeeshan, M., Khan, M.Y., Shahid, M., 2022. Metal organic frameworks (MOFs) as a cutting-edge tool for the selective detection and rapid removal of heavy metal ions from water: Recent progress. *J. Environ. Chem. Eng.* 10, 106991.
- Sheikhsamany, R., Faghihian, H., Fazaeli, R., 2021. One-pot Synthesis of BaTi<sub>0.85</sub>Zr<sub>0.15</sub>O<sub>3</sub>/MOF-199 (HKUST-1) as a highly efficient photocatalytic nanocomposite for tetracycline degradation under UV irradiation. *Inorg. Chem. Commun.*, 109048.
- Shi, Z., Xu, C., Guan, H., Li, L., Fan, L., Wang, Y., Liu, L., Meng, Q., Zhang, R., 2018. Magnetic metal organic frameworks (MOFs) composite for removal of lead and malachite green in wastewater. *Colloids Surf., A* 539, 382–390.
- Singh, S., Kaushal, S., Kaur, J., Kaur, G., Mittal, S.K., Singh, P.P., 2021. CaFu MOF as an efficient adsorbent for simultaneous removal of imidacloprid pesticide and cadmium ions from wastewater. *Chemosphere* 272, 129648.
- Soltani, R., Pelalak, R., Pishnamazi, M., Marjani, A., Shirazian, S., 2021. A water-stable functionalized NiCo-LDH/MOF nanocomposite: green synthesis, characterization, and its environmental application for heavy metals adsorption. *Arabian J. Chem.* 14, 103052.
- Soylak, M., Acar, D., ALOthman, Z., 2017. Activated Carbon Cloth (ACC) as Efficient Adsorbent for Trace Cu (II), Co (II), Cd (II), Pb (II), Mn (II), and Ni (II) as OO-diethylphosphorodithioic Acid Chelates for the Enrichment From Water and Soil Samples.
- Srinivasan, S., Demirocak, D.E., Kaushik, A., Sharma, M., Chaudhary, G.R., Hickman, N., Stefanakos, E., 2020. Reversible hydrogen storage using nanocomposites. *Appl. Sci.* 10, 4618.
- Subramaniam, V., Thangadurai, T.D., Lee, Y.I., 2022. Zirconium based metal-organic framework for the adsorption of Cu (II) ions in real water samples. *Cleaner Eng. Technol.* 9, 100526.
- Sun, D.T., Peng, L., Reeder, W.S., Moosavi, S.M., Tiana, D., Britt, D.K., Oveisi, E., Queen, W.L., 2018. Rapid, Selective Heavy Metal Removal from Water by a Metal-Organic Framework/Polydopamine Composite. *ACS Cent. Sci.* 4, 349–356.
- Tanihara, A., Kikuchi, K., Konno, H., 2021. Insight into the mechanism of heavy metal removal from water by monodisperse ZIF-8 fine particles. *Inorg. Chem. Commun.* 131, 108782.
- Tian, P., He, X., Li, W., Zhao, L., Fang, W., Chen, H., Zhang, F., Zhang, W., Wang, W., 2018. Zr-MOFs based on Keggin-type polyoxometalates for photocatalytic hydrogen production. *J. Mater. Sci.* 53, 12016–12029.
- Tian, X., Yang, R., Chen, T., Cao, Y., Deng, H., Zhang, M., Jiang, X., 2022. Removal of both anionic and cationic dyes from wastewater using pH-responsive adsorbents of L-lysine molecular-grafted cellulose porous foams. *J. Hazard. Mater.* 426, 128121.
- Tokay, B., Akpınar, I., 2021. A comparative study of heavy metals removal using agricultural waste biosorbents. *Bioresour. Technology Reports* 15, 100719.
- Tong, S., Li, H., Tudi, M., Yuan, X., Yang, L., 2021. Comparison of characteristics, water quality and health risk assessment of trace elements in surface water and groundwater in China. *Ecotoxicol. Environ. Saf.* 219, 112283.

- Uddin, M.J., Jeong, Y.-K., 2021. Urban river pollution in Bangladesh during last 40 years: potential public health and ecological risk, present policy, and future prospects toward smart water management. *Heliyon* 7, e06107.
- USGS, 2021. U.S. Geological Survey. <https://www.usgs.gov/centers/nmic/commodity-statistics-and-information> Accessed: November 11, 2021.
- Vilela, S.M.F., Navarro, J.A.R., Barbosa, P., Mendes, R.F., Pérez-Sánchez, G., Nowell, H., Ananias, D., Figueiredo, F., Gomes, J.R.B., Tomé, J.P.C., Paz, F.A.A., 2021. Multifunctionality in an Ion-Exchanged Porous Metal-Organic Framework. *J. Am. Chem. Soc.* 143, 1365–1376.
- Wang, Y., Bi, F., Wang, Y., Jia, M., Tao, X., Jin, Y., Zhang, X., 2021a. MOF-derived CeO<sub>2</sub> supported Ag catalysts for toluene oxidation: The effect of synthesis method. *Molecular Catalysis* 515, 111922.
- Wang, Z., Cohen, S.M., 2009. Postsynthetic modification of metal-organic frameworks. *Chem. Soc. Rev.* 38, 1315–1329.
- Wang, K., Gu, J., Yin, N., 2017. Efficient removal of Pb (II) and Cd (II) using NH<sub>2</sub>-functionalized Zr-MOFs via rapid microwave-promoted synthesis. *Ind. Eng. Chem. Res.* 56, 1880–1887.
- Wang, Y., Li, M., Hu, J., Feng, W., Li, J., You, Z., 2021b. Highly efficient and selective removal of Pb<sup>2+</sup> by ultrafast synthesis of HKUST-1: Kinetic, isotherms and mechanism analysis. *Colloids Surfaces A: Physicochem. Eng. Aspects*, 127852.
- Wang, C., Liu, X., Chen, J.P., Li, K., 2015a. Superior removal of arsenic from water with zirconium metal-organic framework UiO-66. *Sci. Rep.* 5, 16613.
- Wang, C., Lin, G., Xi, Y., Li, X., Huang, Z., Wang, S., Zhao, J., Zhang, L., 2020a. Development of mercaptosuccinic anchored MOF through one-step preparation to enhance adsorption capacity and selectivity for Hg(II) and Pb(II). *J. Mol. Liq.* 317, 113896.
- Wang, C., Lin, G., Zhao, J., Wang, S., Zhang, L., Xi, Y., Li, X., Ying, Y., 2020b. Highly selective recovery of Au (III) from wastewater by thioctic acid modified Zr-MOF: Experiment and DFT calculation. *Chem. Eng. J.* 380, 122511.
- Wang, Y., Lin, K., Liu, Y., Deng, X., 2022b. Nanocomposites of functionalized Metal–Organic frameworks and magnetic graphene oxide for selective adsorption and efficient determination of Lead (II). *J. Solid State Chem.* 313, 123300.
- Wang, K., Tian, Z., Yin, N., 2018. Significantly Enhancing Cu(II) Adsorption onto Zr-MOFs through Novel Cross-Flow Disturbance of Ceramic Membrane. *Ind. Eng. Chem. Res.* 57, 3773–3780.
- Wang, N., Xie, J., Zhang, J., 2022a. MOF-253 immobilized Pd and Cu as recyclable and efficient green catalysts for Sonogashira reaction. *Arabian J. Chem.* 15, 103962.
- Wang, Y., Ye, G., Chen, H., Hu, X., Niu, Z., Ma, S., 2015b. Functionalized metal-organic framework as a new platform for efficient and selective removal of cadmium(ii) from aqueous solution. *J. Mater. Chem. A* 3, 15292–15298.
- Wang, X., Zhu, H., Sun, T., Dai, H., 2020c. Synthesis of a Matériaux Institut Lavoisier metal-organic framework 96 (MIL-96(RM)) using red mud and its application to defluorination of water. *Mater. Today Commun.* 25, 101401.
- Wen, J., Hu, X., 2021. Metal selectivity and effects of co-existing ions on the removal of Cd, Cu, Ni, and Cr by ZIF-8-EGCG nanoparticles. *J. Colloid Interface Sci.* 589, 578–586.
- Wu, N., Guo, H., Xue, R., Wang, M., Cao, Y., Wang, X., Xu, M., Yang, W., 2021. A free nitrogen-containing Sm-MOF for selective detection and facile removal of mercury(II). *Colloids Surf., A* 618, 126484.
- Wu, Q., Wang, S., Wang, L., Liu, F., Lin, C.-J., Zhang, L., Wang, F., 2014. Spatial distribution and accumulation of Hg in soil surrounding a Zn/Pb smelter. *Sci. Total Environ.* 496, 668–677.
- Wu, J., Zhou, J., Zhang, S., Alsaedi, A., Hayat, T., Li, J., Song, Y., 2019. Efficient removal of metal contaminants by EDTA modified MOF from aqueous solutions. *J. Colloid Interface Sci.* 555, 403–412.
- Xiong, C., Wang, S., Hu, P., Huang, L., Xue, C., Yang, Z., Zhou, X., Wang, Y., Ji, H., 2020. Efficient selective removal of Pb (II) by using 6-aminothiouracil-modified Zr-based organic frameworks: from experiments to mechanisms. *ACS Appl. Mater. Interfaces* 12, 7162–7178.
- Xu, R., Jian, M., Ji, Q., Hu, C., Tang, C., Liu, R., Zhang, X., Qu, J., 2020. 2D water-stable zinc-benzimidazole framework nanosheets for ultrafast and selective removal of heavy metals. *Chem. Eng. J.* 382, 122658.
- Xu, L., Wang, T., Wang, J., Lu, A., 2017. Occurrence, speciation and transportation of heavy metals in 9 coastal rivers from watershed of Laizhou Bay, China. *Chemosphere* 173, 61–68.
- Xue, H., Chen, Q., Jiang, F., Yuan, D., Lv, G., Liang, L., Liu, L., Hong, M., 2016. A regenerative metal-organic framework for reversible uptake of Cd (II): from effective adsorption to in situ detection. *Chem. Sci.* 7, 5983–5988.
- Yan, Y., Chu, Y., Khan, M.A., Xia, M., Shi, M., Zhu, S., Lei, W., Wang, F., 2022. Facile immobilization of ethylenediamine tetramethylene-phosphonic acid into UiO-66 for toxic divalent heavy metal ions removal: An experimental and theoretical exploration. *Sci. Total Environ.* 806, 150652.
- Yazdi, M.N., Dadfarnia, S., Shabani, A.M.H., 2021. Synthesis of stable S-functionalized metal-organic framework using MoS<sub>4</sub>2- and its application for selective and efficient removal of toxic heavy metal ions in wastewater treatment. *J. Environ. Chem. Eng.* 9, 104696.
- Yin, N., Wang, K., Li, Z., 2018. Novel melamine modified metal-organic frameworks for remarkably high removal of heavy metal Pb (II). *Desalination* 430, 120–127.
- You, D., Shi, H., Peng, M., Yang, L., Shao, P., Yin, K., Wang, H., Luo, S., Luo, X., 2022. Metal-center effect induced efficient charge transfer of metal-organic framework for strengthening Sb(V) capture performance. *Nano Res.*
- Yuan, G., Tian, Y., Liu, J., Tu, H., Liao, J., Yang, J., Yang, Y., Wang, D., Liu, N., 2017. Schiff base anchored on metal-organic framework for Co (II) removal from aqueous solution. *Chem. Eng. J.* 326, 691–699.
- Yuan, Q., Wang, Y., Yuan, F., Jia, S., Sun, H., Zhang, X., 2022a. Water-stable metal organic framework-199@polyaniline with high-performance removal of copper II. *Environ. Sci. Pollut. Res.* 29, 44883–44892.
- Yuan, X., Xue, N., Han, Z., 2021. A meta-analysis of heavy metals pollution in farmland and urban soils in China over the past 20 years. *J. Environ. Sci.* 101, 217–226.
- Yuan, Y., Yu, J., Chen, H., Bang, K.-T., Pan, D., Kim, Y., 2022b. Thiol-functionalized Zr metal-organic frameworks for efficient removal of Fe<sup>3+</sup> from water. *Cell Reports Phys. Sci.* 3, 100783.
- Yusuf, K., Shekhah, O., AlOthman, Z., Eddaoudi, M., 2021. Metal-Organic Frameworks Characterization via Inverse Pulse Gas Chromatography. *Appl. Sci.* 11, 10243.
- Zhang, H., Hu, X., Li, T., Zhang, Y., Xu, H., Sun, Y., Gu, X., Gu, C., Luo, J., Gao, B., 2022b. MIL series of metal organic frameworks (MOFs) as novel adsorbents for heavy metals in water: A review. *J. Hazard. Mater.* 429, 128271.
- Zhang, L., Xu, Y., Liu, H., Li, Y., You, S., Zhao, J., Zhang, J., 2021a. Effects of coexisting Na<sup>+</sup>, Mg<sup>2+</sup> and Fe<sup>3+</sup> on nitrogen and phosphorus removal and sludge properties using A2O process. *J. Water Process Eng.* 44, 102368.
- Zhang, L., Wang, L., Zhang, Y., Wang, D., Guo, J., Zhang, M., Li, Y., 2022c. The performance of electrode ultrafiltration membrane bioreactor in treating cosmetics wastewater and its anti-fouling properties. *Environ. Res.* 206, 112629.
- Zhang, C., Zhai, M., Xie, K., Wang, Y., Li, X., Liu, J., Li, Y., Hu, Y., Luo, E., Tang, C., 2022a. Enhanced alcohol and H<sub>2</sub>O adsorption and separation performances by introducing pyridyl ligand in a MOF. *Arabian J. Chem.* 15, 104141.
- Zhang, Y., Zheng, H., Zhang, P., Zheng, X., Zuo, Q., 2021b. A facile method to achieve dopamine polymerization in MOFs pore

- structure for efficient and selective removal of trace lead (II) ions from drinking water. *J. Hazard. Mater.* 408, 124917.
- Zhao, M., Huang, Z., Wang, S., Zhang, L., Wang, C., 2020b. Experimental and DFT study on the selective adsorption mechanism of Au (III) using amidinothiourea-functionalized UiO-66-NH<sub>2</sub>. *Microporous Mesoporous Mater.* 294, 109905.
- Zhao, M., Huang, Z., Wang, S., Zhang, L., Wang, C., 2020c. Experimental and DFT study on the selective adsorption mechanism of Au(III) using amidinothiourea-functionalized UiO-66-NH<sub>2</sub>. *Microporous Mesoporous Mater.* 294, 109905.
- Zhao, J., Wang, C., Wang, S., Zhou, Y., 2020a. Experimental and DFT study of selective adsorption mechanisms of Pb (II) by UiO-66-NH<sub>2</sub> modified with 1, 8-dihydroxyanthraquinone. *J. Ind. Eng. Chem.* 83, 111–122.
- Zhao, X., Yu, X., Wang, X., Lai, S., Sun, Y., Yang, D., 2021. Recent advances in metal-organic frameworks for the removal of heavy metal oxoanions from water. *Chem. Eng. J.* 407, 127221.
- Zheng, Y., Rao, F., Zhang, M., Li, J., Huang, W., 2021. Efficient, selective, and reusable metal-organic framework-based adsorbent for the removal of Pb(II) and Cr(VI) heavy-metal pollutants from wastewater. *Cleaner Eng. Technol.* 5, 100344.
- Zhou, X., Liang, Q., Yang, B., Chen, Y., Fang, Y., Luo, H., Liu, Y., 2020b. Rational design an amorphous multifunctional  $\delta$ -MnO<sub>2</sub>@Fe/Mg-MIL-88B nanocomposites with tailored components for efficient and rapid removal of arsenic in water. *Colloids Surf., A* 602, 125141.
- Zhou, Q., Yang, N., Li, Y., Ren, B., Ding, X., Bian, H., Yao, X., 2020a. Total concentrations and sources of heavy metal pollution in global river and lake water bodies from 1972 to 2017. *Global Ecol. Conserv.* 22, e00925.
- Zhu, J., Wu, L., Bu, Z., Jie, S., Li, B.-G., 2019b. Polyethyleneimine-Modified UiO-66-NH<sub>2</sub>(Zr) Metal-Organic Frameworks: Preparation and Enhanced CO<sub>2</sub> Selective Adsorption. *ACS Omega* 4, 3188–3197.
- Zhu, X.-H., Yang, C.-X., Yan, X.-P., 2018. Metal-organic framework-801 for efficient removal of fluoride from water. *Microporous Mesoporous Mater.* 259, 163–170.
- Zhu, H., Yuan, J., Tan, X., Zhang, W., Fang, M., Wang, X., 2019a. Efficient removal of Pb<sup>2+</sup> by Tb-MOFs: identifying the adsorption mechanism through experimental and theoretical investigations. *Environ. Sci. Nano* 6, 261–272.
- Zuhra, Z., Ali, S., Ali, S., Xu, H., Wu, R., Tang, Y., 2021. Exceptionally amino-quantitated 3D MOF@CNT-sponge hybrid for efficient and selective recovery of Au(III) and Pd(II). *Chem. Eng. J.*, 133367